Tetrachloro- and Tetrabromostibonium(V) Cations: Raman and ^{19}F, ^{121}Sb, and ^{123}Sb NMR Spectroscopic Characterization and X-ray Crystal Structures of $SbCl_4^+Sb(OTeF_5)_6^-$ and $SbBr_4^+Sb(OTeF_5)_6^-$

William J. Casteel, Jr., Peter Kolb, Nicolas LeBlond, Hélène P. A. Mercier, and Gary J. Schrobilgen*

Department of Chemistry, McMaster University, Hamilton, Ontario L8S 4M1, Canada

Received June 30, 1995[⊗]

The stable salts, $SbCl_4^+Sb(OTeF_5)_6^-$ and $SbBr_4^+Sb(OTeF_5)_6^-$, have been prepared by oxidation of $Sb(OTeF_5)_3$ with Cl_2 and Br_2, respectively. The $SbBr_4^+$ cation is reported for the first time and is only the second example of a tetrahalostibonium(V) cation. The $SbCl_4^+$ cation had been previously characterized as the $Sb_2F_{11}^-$, $Sb_2Cl_2F_9^-$, and $Sb_2Cl_{0.5}F_{10.5}^-$ salts. Both $Sb(OTeF_5)_6^-$ salts have been characterized in the solid state by low-temperature Raman spectroscopy and X-ray crystallography. Owing to the weakly coordinating nature of the $Sb(OTeF_5)_6^-$ anion, both salts are readily soluble in SO_2ClF and have been characterized in solution by ^{121}Sb, ^{123}Sb, and ^{19}F NMR spectroscopy. The tetrahedral environments around the Sb atoms of the cations result in low electric field gradients at the quadrupolar ^{121}Sb and ^{123}Sb nuclei and correspondingly long relaxation times, allowing the first solution NMR characterization of a tetrahalocation of the heavy pnicogens. The following crystal structures are reported: $SbCl_4^+Sb(OTeF_5)_6^-$, trigonal system, space group $P\bar{3}$, $a = 10.022(1)$ Å, $c = 18.995(4)$ Å, $V = 1652.3(6)$ Å^3, $D_{calc} = 3.652$ g cm^{-3}, $Z = 2$, $R_1 = 0.0461$; $SbBr_4^+Sb(OTeF_5)_6^-$, trigonal system, space group $P\bar{3}$, $a = 10.206(1)$ Å, $c = 19.297(3)$ Å, $V = 1740.9(5)$ Å^3, $D_{calc} = 3.806$ g cm^{-3}, $Z = 2$, $R_1 = 0.0425$. The crystal structures of both $Sb(OTeF_5)_6^-$ salts are similar and reveal considerably weaker interactions between anion and cation than in previously known $SbCl_4^+$ salts. Both cations are undistorted tetrahedra with bond lengths of 2.221(3) Å for $SbCl_4^+$ and 2.385(2) Å for $SbBr_4^+$. The Raman spectra are consistent with undistorted SbX_4^+ tetrahedra and have been assigned under T_d point symmetry. Trends within groups 15 and 17 are noted among the general valence force constants of the PI_4^+, AsF_4^+, $AsBr_4^+$, AsI_4^+, $SbCl_4^+$ and $SbBr_4^+$ cations, which have been calculated for the first time, and the previously determined force constants for NF_4^+, NCl_4^+, PF_4^+, PCl_4^+, PBr_4^+, and $AsCl_4^+$, which have been recalculated for the P and As cations in the present study. The $SbCl_4^+$ salt is stable in SO_2ClF solution, whereas the $SbBr_4^+$ salt decomposes slowly in SO_2ClF at room temperature and rapidly in the presence of Br^- ion and in CH_3CN solution at low temperatures. The major products of the decompositions are $SbBr_2^+Sb(OTeF_5)_6^-$, as an adduct with CH_3CN in CH_3CN solvent, and Br_2.

Introduction

Although the nonmetals of the fourth row of the periodic table are unstable in their highest oxidation state,[1,2] the entire series of tetrahaloarsonium(V) cations, AsF_4^+,[3] $AsCl_4^+$,[4−6] $AsBr_4^+$,[7] and AsI_4^+,[8] are now known as well as their tetrahalophosphonium(V) analogs,[9−16] NF_4^+ [17,18] and NCl_4^+.[19] The only tetrahalostibonium(V) cation reported and characterized to date is the $SbCl_4^+$ cation,[20−23] and no example of a bismuth analog is presently known.

Synthetic approaches yielding salts containing the $SbCl_4^+$ cations have been known for some time. The reactions of $SbCl_5$ with AsF_3[24] or ClF with $SbCl_5$[25] yield $SbCl_4F$ which was originally formulated as $SbCl_4^+F^-$ on the basis of its low-gain Raman spectrum.[25] The structure of $SbCl_4F$ was subsequently shown to be a fluorine-bridged tetramer,[26] and the Raman spectrum has been reinterpreted in terms of this structure.[27] The oxidation of SbF_3 with Cl_2,[28] or reaction of $SbCl_5$ with ClF_3,[29]

[⊗] Abstract published in *Advance ACS Abstracts,* January 1, 1996.

(1) Huheey, J. E. *Inorganic Chemistry*, 3rd ed.; Harper and Row: Philadelphia, PA, 1983; p 841.
(2) Greenwood, N. N.; Earnshaw, A. *Chemistry of the Elements*; Pergamon Press: Oxford, England, 1984; p 644.
(3) Broschag, M.; Klapötke, T.; Tornieporth-Oetting, I. C. *J. Chem. Soc., Chem. Commun.* **1992**, 446.
(4) Minkwitz, R.; Nowicki, J.; Borrmann, H. *Z. Anorg. Allg. Chem.* **1991**, *596*, 93.
(5) Preiss, H. *Z. Anorg. Allg. Chem.* **1971**, *380*, 71.
(6) (a) Weidlein, J.; Dehnicke, K. *Z. Anorg. Allg. Chem.* **1965**, *337*, 113. (b) Kolditz, L. *Z. Anorg. Allg. Chem.* **1955**, *280*, 313.
(7) Klapötke, T.; Passmore, J. *J. Chem. Soc., Dalton Trans.* **1990**, 3815.
(8) Tornieporth-Oetting, I.; Klapötke, T. *Angew. Chem., Int. Ed. Engl.* **1989**, *28*, 1671.
(9) Chen, G. S. H.; Passmore, J. *J. Chem. Soc., Dalton Trans.* **1979**, 1251.
(10) (a) Minkwitz, R.; Liedtke, A. *Z. Naturforsch. B* **1989**, *44*, 679. (b) Minkwitz, R.; Lennhoff, D.; Sawodny, W.; Härtner, H. *Z. Naturforsch. B* **1992**, *47*, 1661.
(11) Van Huong, P.; Debat, B. *Bull. Soc. Chim. Fr.* **1972**, 2631.
(12) Erdbrügger, C. F.; Jones, P. G.; Schelbach, R.; Schwarzmann, E.; Sheldrick, G. M. *Acta Crystallogr.* **1987**, *C43*, 1857.
(13) Breneman, G. L.; Willet, R. D. *Acta Crystallogr.* **1967**, *23*, 467.
(14) Delahaye, M.; Dhamelincourt, P.; Merlin, V. C. *C. R. Acad. Sci. Ser. B* **1971**, *272*, 370.
(15) Pohl, S. *Z. Anorg. Allg. Chem.* **1983**, *15*, 498.
(16) Tornieporth-Oetting, I.; Klapötke, T. *J. Chem. Soc., Chem. Commun.* **1990**, 132.
(17) Christe, K. O. *Spectrochim. Acta* **1980**, *36A*, 921.
(18) Christe, K. O.; Lindt, M. D.; Thorup, N.; Russell, D. R.; Fawcett, J.; Bau, R. *Inorg. Chem.* **1988**, *27*, 2450.
(19) Minkwitz, R.; Bernstein, D.; Sawodny, W. *Angew. Chem., Int. Ed. Engl.* **1990**, *29*, 181.
(20) Preiss, H. *Z. Anorg. Allg. Chem.* **1972**, *389*, 254.
(21) Miller, H. B.; Baird, H. W.; Bramlett, C. L.; Templeton, W. K. *J. Chem. Soc., Chem. Commun.* **1972**, 262.
(22) Müller, U. *Z. Naturforsch.* **1979**, *34B*, 681.
(23) Birchall, T.; Ballard, J. G. *Can. J. Chem.* **1978**, *56*, 2947.
(24) Kolditz, L. *Z. Anorg. Allg. Chem.* **1956**, *284*, 144.
(25) Dehnicke, K.; Weidlein, *J. Chem. Ber.* **1965**, *98*, 1087.
(26) Preiss, H. *Z. Chem.* **1966**, *6*, 350.
(27) Beattie, I. R.; Livingston, K. M. S.; Ozin, G. A.; Reynolds, D. J. *J. Chem. Soc. A* **1969**, 958.
(28) Kolditz, L.; von der Lieth, W. *Z. Anorg. Allg. Chem.* **1961**, *310*, 236.

0020-1669/96/1335-0929$12.00/0

has yielded a product having the stoichiometry $SbCl_2F_3$. Although conductivity measurements and the existence of the $PCl_4^+PF_6^-$ and $AsCl_4^+AsF_6^-$ salts suggested an ionic formulation, $SbCl_4^+SbF_6^-$,[28] a subsequent vibrational spectroscopic study wrongly concluded that the compound had the molecular formula, $SbCl_2F_3$ (D_{3h} point symmetry).[29] Fluorine-19 NMR spectroscopy suggested an associated species containing hexacoordinated antimony.[30] The crystal structure subsequently revealed an ionic structure, $SbCl_4^+Sb_2Cl_2F_9^-$, with a fluorine-bridged anion.[20] Two other $SbCl_4^+$ salts, $SbCl_4^+Sb_2F_{11}^-$ [21] and $SbCl_4^+Sb_2Cl_{0.5}F_{10.5}^-$,[22] have been isolated from $SbCl_5/SbF_5$ mixtures containing stoichiometric excesses of SbF_5 and characterized by single-crystal X-ray diffraction. Both salts are isostructural with $SbCl_4^+Sb_2Cl_2F_9^-$. Although the Raman spectrum of $SbCl_4^+Sb_2Cl_2F_9^-$ was correctly reinterpreted as a result of the X-ray analysis, one of the Raman bands of $SbCl_4^+$, ν_2(E), was not detected.[20] The Raman spectra of the $SbCl_4^+$ cations in $SbCl_4^+Sb_2F_{11}^-$ and $SbCl_4^+Sb_2Cl_2F_9^-$ have since been fully assigned.[23] The $SbCl_4^+SbF_6^-$ and $SbCl_4^+AsF_6^-$ salts are unknown. It is interesting to note that the stoichiometry of $SbCl_2F_3$ can either correspond to 3 mol of $SbCl_4^+SbF_6^-$ or to 2 mol of $SbCl_4^+Sb_2Cl_2F_9^-$, indicating that $SbCl_4^+SbF_6^-$ is thermally unstable with respect to $SbCl_4^+Sb_2Cl_2F_9^-$. In an attempt to prepare the $SbCl_4^+AsF_6^-$ salt by reaction of $SbCl_4F$ and AsF_5, it was found that halogen redistribution occurred to give $AsCl_4^+SbF_6^-$.[23]

The tetrahaloarsonium(V) cations have been synthesized as the $AsF_4^+PtF_6^-$,[3] $AsCl_4^+AsF_6^-$,[4-6] $AsBr_4^+AsF_6^-$,[7] $AsBr_4^+AlBr_4^-$/$Al_2Br_7^-$,[7] and $AsI_4^+AlCl_4^-$ [8] salts. The $AsBr_4^+$ and AsI_4^+ salts are thermodynamically and kinetically unstable, decomposing at −78 °C, whereas $AsF_4^+PtF_6^-$ and $AsCl_4^+AsF_6^-$ are thermodynamically stable. The $AsBr_4^+$ and AsI_4^+ salts have been characterized at low temperature by solid state Raman spectroscopy, and their relative stabilities have been rationalized on the basis of simple Born−Haber cycles.[7,8] Possible decomposition mechanisms have been proposed, in particular for the $AsBr_4^+AsF_6^-$ salt. The initiating step likely involves fluoride ion transfer from the anion to the cation. The proposed intermediate, "$AsBr_4^+F^-$", is expected to be kinetically unstable, decomposing to Br_2 and $AsBr_2F$. The latter compound may undergo rapid halogen exchange to yield AsF_3 and $AsBr_3$ or be oxidized by AsF_5 to yield AsF_3 and Br_2. Arsenic trifluoride and Br_2 were consistently obtained as the final products, and $AsBr_3$ was detected as an intermediate. Raman spectroscopic evidence also indicates that the $AsBr_4^+$ cation is stabilized at low temperatures as a mixture of $AlBr_4^-$ and $Al_2Br_7^-$ salts. The salt $AsCl_3F^+AsF_6^-$ [31] has recently been synthesized by oxidative fluorination of $AsCl_3$ with $XeF^+AsF_6^-$ in HF solvent at −80 °C, but could not be obtained as a pure product. The salt is stable in the solid state at −60 °C, but undergoes F^- transfer in HF solution to yield AsF_5 and $AsCl_4^+AsF_6^-$. The $AsCl_4^+$ cation in $AsCl_4^+AsF_6^-$ [4] and $AsCl_4^+SbCl_6^-\cdot AsCl_3$[5] is the only tetrahaloarsonium cation to have been characterized by X-ray crystallography.

Although $PI_4^+AlI_4^-$ is thermodynamically stable and has been characterized by X-ray crystallography,[15] the recently synthesized salts, $PI_4^+AsF_6^-$ and $PI_4^+SbF_6^-$, are thermodynamically and kinetically unstable and likely decompose in a manner similar to $AsBr_4^+AsF_6^-$, since the AsF_6^- salt yields the corresponding products AsF_3, PF_3, and I_2.[16] Interestingly, the salt $PBr_4^+PF_6^-$ was estimated to be only marginally stable with respect to decomposition to PF_5, PBr_3, and Br_2,[7] but it is found to be stable up to 135 °C.[32] Moreover, this salt reacts only slowly with AsF_3, whereas $PCl_4^+PF_6^-$ is readily converted into PF_5 and $AsCl_3$,[32] indicating a marked degree of kinetic stabilization. The kinetic instability of the $AsBr_4^+$ and PI_4^+ cations in their AsF_6^- salts has prevented their characterization by any technique other than low-temperature Raman spectroscopy.

While the $AsBr_4^+$ cation has been synthesized as a thermally unstable AsF_6^- salt and the $SbBr_6^-$ anion and several examples of adducts of unknown $SbBr_5$ exist, the $SbBr_4^+$ cation has thus far eluded synthesis and characterization. The inability to synthesize $SbBr_5$ from Br_2 and $SbBr_3$[33] and the thermal instabilities of $PI_4^+AsF_6^-$, $AsCl_3F^+AsF_6^-$, $AsBr_4^+AsF_6^-$, and $AsI_4^+AlI_4^-$, along with their observed decomposition products, suggest that coordination of the anion with the cation to give a pentacoordinate pnicogen center may be important in the kinetic destabilization of a number of the heavy PnX_4^+ cations. Suitably weakly coordinating and oxidatively resistant anions such as the $Pn(OTeF_5)_6^-$ anions (Pn = As, Sb, Bi), which have recently been characterized in this laboratory,[34] may offer prospects for the synthesis of salts of the strongly Lewis acidic tetrahalostibonium(V) cations. Because the charge of a $Pn(OTeF_5)_6^-$ anion is dispersed over 30 rather than six fluorines, as in the PnF_6^- anions, and access to the lone electron pairs of the oxygens is inhibited by the octahedral coordination, the cations are expected to interact weakly with the $Pn(OTeF_5)_6^-$ anion. The low basicities of the $Pn(OTeF_5)_6^-$ anions may reasonably be expected to play a role in the kinetic stabilization of PnX_4^+ species and inhibit F^- and $OTeF_5^-$ anion coordination, transfer, and decomposition by means of mechanisms analogous to those proposed for $AsBr_4^+AsF_6^-$, $PI_4^+AsF_6^-$ and $AsI_4^+AlI_4^-$.

The present paper describes facile syntheses of stable compounds of both the $SbCl_4^+$ cation and novel $SbBr_4^+$ cation as their $Sb(OTeF_5)_6^-$ salts and their structural characterization in solution by ^{19}F, ^{121}Sb, and ^{123}Sb NMR spectroscopy and in the solid state by X-ray crystallography and Raman spectroscopy. The $Sb(OTeF_5)_6^-$ salt of the known $SbCl_4^+$ cation is also of interest, since the published crystal structures either have not been fully refined and/or are of low precision.[20-22]

Results and Discussion

Synthesis of $SbCl_4^+Sb(OTeF_5)_6^-$ and $SbBr_4^+Sb(OTeF_5)_6^-$. Both tetrastibonium(V) salts were obtained according to eq 1

$$2Sb(OTeF_5)_3 + 2X_2 \xrightarrow[\text{several days}]{\text{room temp}} SbX_4^+Sb(OTeF_5)_6^- \quad (1)$$

where X = Cl or Br. The reactions proceeded at ambient temperature in the liquid state in the absence of a solvent because the low melting point of $Sb(OTeF_5)_3$ (39 °C) is depressed sufficiently by dissolved halogen to give a liquid mixture at room temperature. The resulting salts have low solubilities in liquid $Sb(OTeF_5)_3$ and crystallize as colorless $SbCl_4^+Sb(OTeF_5)_6^-$ or yellow $SbBr_4^+Sb(OTeF_5)_6^-$ salts which are stable indefinitely at room temperature. In both cases, suitable crystals for single-crystal X-ray structure determinations could be obtained directly from the reaction mixtures. An attempt to prepare $SbI_4^+Sb(OTeF_5)_6^-$ by an analogous route, $Sb(OTeF_5)_3$ and I_2, failed over a period of several weeks at room temperature.

Both salts are stable solids at room temperature, and the $SbCl_4^+$ salt is stable in SO_2ClF and CH_3CN solvents at room temperature. The stability of $SbCl_4^+Sb(OTeF_5)_6^-$ in CH_3CN

(29) Dehnicke, K.; Weidlein, J. *Z. Anorg. Allg. Chem.* **1963**, *323*, 267.
(30) Muetterties, E. L.; Mahler, W.; Packer, K. J.; Schmutzler, R. *Inorg. Chem.* **1964**, *3*, 1298.
(31) Minkwitz, R.; Molsbeck, W. *Z. Anorg. Allg. Chem.* **1992**, *607*, 175.
(32) Feltz, A.; Kolditz, L. *Z. Anorg. Allg. Chem.* **1957**, *293*, 155.
(33) Holmes, R. R. *J. Inorg. Nucl. Chem.* **1961**, *19*, 363.
(34) Mercier, H. P. A.; Sanders, J. C. P.; Schrobilgen, G. J. *J. Am. Chem. Soc.* **1994**, *116*, 2921.

Table 1. ^{121}Sb and ^{123}Sb NMR Parameters[a] for $SbCl_4^+Sb(OTeF_5)_6^-$ and $SbBr_4^+Sb(OTeF_5)_6^-$

		chem shifts, ppm				
		$B_o = 7.0463$ T[b]		$B_o = 11.7440$ T[b]		
solute[c]	ion	$\delta(^{121}Sb)$	$\delta(^{123}Sb)$	$\delta(^{121}Sb)$	$\delta(^{123}Sb)$	$\Delta\nu_{1/2}(^{121}Sb)/\Delta\nu_{1/2}(^{123}Sb)$
$SbCl_4^+Sb(OTeF_5)_6^-$	$SbCl_4^+$	760.4 (2770)	759.4 (1990)			1.39
	$Sb(OTeF_5)_6^-$	−13.7 (1210)	−13.4 (784)			1.54
$SbBr_4^+Sb(OTeF_5)_6^-$	$SbBr_4^+$	8.7 (865)	3.9 (650)	8.6 (890)	3.9 (615)	1.45[d]
	$Sb(OTeF_5)_6^-$	−13.5 (1120)	−12.8 (670)	−13.6 (1060)	−13.6 (690)	1.53[d]

[a] Chemical shifts were referenced externally relative to 1.0 M $N(CH_2CH_3)_4^+SbF_6^-$ in CH_3CN at the sample temperature. [b] Line widths, $\Delta\nu_{1/2}$, in Hz are given in parentheses. [c] Spectra were recorded in SO_2ClF solvent at 27 °C. [d] The cation and anion lines severely overlap at $B_o = 7.0463$ T; values reported are for $B_o = 11.744$ T.

solution contrasts with an earlier report that $SbCl_4^+SbF_6^-$ slowly attacked CH_3CN;[35] the nature of the decomposition and the resulting products were not discussed. The same report notes that $SbCl_4^+SbF_6^-$ was recovered unchanged from liquid SO_2, although conductivity studies led to the speculation that $SbCl_4^+SbF_6^-$ was in equilibrium with "$SbCl_2F_3$" in SO_2 solution (latter shown to be $SbCl_4^+Sb_2Cl_2F_9^-$ [20]).

Solution NMR samples of the $SbBr_4^+$ salt, prepared in the weakly coordinating solvent SO_2ClF, changed in color from pale yellow to light orange, and the $SbBr_4^+$ resonance slightly decreased relative to that of the $Sb(OTeF_5)_6^-$ anion, after running the spectra, indicating partial decomposition with liberation of Br_2. Allowing an SO_2ClF solution of $SbBr_4^+Sb(OTeF_5)_6^-$ to stand for 8 days at room temperature resulted in incomplete decomposition with loss of Br_2 as indicated by the ^{19}F NMR and Raman spectra of the isolated product (see **Experimental Section**). In the more strongly coordinating solvent, CH_3CN, the decomposition was rapid near the melting point of the solvent (−45 °C) and is consistent with eq 2. The presence of

$$SbBr_4^+Sb(OTeF_5)_6^- \xrightarrow[CH_3CN]{-45\ ^\circ C} (SbBr_2^+\cdot xCH_3CN)Sb(OTeF_5)_6^- + Br_2 \quad (2)$$

the $Sb(OTeF_5)_6^-$ anion was demonstrated by recording the NMR spectra of a decomposed sample in CH_3CN which gave ^{19}F, ^{121}Sb, and ^{123}Sb spectra in agreement with those obtained previously.[34] The intense red-orange color change and its removal under dynamic vacuum at room temperature was a clear indication of Br_2 formation. The ^{19}F NMR spectrum of a decomposed sample, redissolved in SO_2ClF, was also consistent with $Sb(OTeF_5)_6^-$ and identical to those obtained for the $SbX_4^+Sb(OTeF_5)_6^-$ salts. The presence of CH_3CN could be shown in the ^{1}H NMR spectrum, where the peak assigned to CH_3CN was found at 2.10 ppm. Although bands corresponding to the C≡N and C−C stretching and CH_3 bending modes of CH_3CN were observed in the low-temperature Raman spectrum, the presence of the $SbBr_2^+$ cation or its adduct with CH_3CN could not be definitively established by Raman spectroscopy (see **Experimental Section**) because the Raman frequencies of the $SbBr_2^+$ cation[36] are nearly coincident with those of $SbBr_3$,[37] which was also found, as single crystals, in the reaction mixture and verified from its unit cell parameters.[38] The formation of $SbBr_3$ indicates that the decomposition does not strictly follow eq 2. It is reasonable to speculate that the initial product of the reaction between $SbBr_4^+$ and CH_3CN is likely an unstable pentacoordinate adduct cation, $SbBr_4^+\cdot CH_3CN$, which rapidly decomposes to $SbBr_2^+\cdot CH_3CN$ and Br_2. This behavior is consistent with the fact that $SbBr_5$ is unknown and cannot be formed from $SbBr_3$ and Br_2.[33] The instability of the $SbBr_4^+$ cation in CH_3CN contrasts with the stability of $SbCl_5$ and solutions of $SbCl_4^+Sb(OTeF_5)_6^-$ in CH_3CN, which shows no signs of decomposition for up to several hours at room temperature (see **NMR Spectroscopy**). It has also been noted that $AsCl_4^+AsF_6^-$ is unstable in the weakly coordinating solvent, SO_2, slowly liberating Cl_2 and AsF_3.[39]

An attempt to form $SbBr_5$ by low-temperature displacement from $SbBr_4^+Sb(OTeF_5)_6^-$ using $N(CH_2CH_3)_4^+Br^-$ in SO_2ClF solution at −78 to −60 °C resulted in rapid Br_2 evolution. The material balance and Raman spectra were consistent with the formation of $N(CH_2CH_3)_4^+Sb(OTeF_5)_6^-$ [34] and $SbBr_3$[37] according to eq 3.

$$SbBr_4^+Sb(OTeF_5)_6^- + N(CH_2CH_3)_4^+Br^- \xrightarrow[SO_2ClF]{-78\ \text{to}\ -60\ ^\circ C} SbBr_3 + N(CH_2CH_3)_4^+Sb(OTeF_5)_6^- + Br_2 \quad (3)$$

Halogen scrambling was investigated for a 1.037:1.000 molar mixture of $SbCl_4^+Sb(OTeF_5)_6^-/SbBr_4^+Sb(OTeF_5)_6^-$ dissolved in SO_2ClF. The mixture was monitored by ^{121}Sb and ^{123}Sb NMR spectroscopy at room temperature and showed the decomposition of the $SbBr_4^+$ cation with Br_2 evolution was essentially 70% complete after three hours and was decidely more rapid than in the absence of $SbCl_4^+$. No mixed $SbCl_{4-x}Br_x^+$ species, which are expected to give rise to quadrupole broadened resonances having chemical shifts intermediate between those of the parent $SbCl_4^+$ and $SbBr_4^+$ cations, were detected (see **NMR Spectroscopy**).

^{19}F, ^{121}Sb, and ^{123}Sb NMR Spectroscopy of $SbX_4^+Sb(OTeF_5)_6^-$ (X = Cl or Br). The ^{121}Sb and ^{123}Sb NMR parameters of $SbX_4^+Sb(OTeF_5)_6^-$ are listed in Table 1 and the ^{121}Sb and ^{123}Sb NMR spectra are depicted in Figures 1 and 2.

The ^{19}F NMR spectra of the $SbX_4^+Sb(OTeF_5)_6^-$ salts recorded at 7.0463 T in SO_2ClF solvent are very similar and display severe second order AB_4 spin patterns and ^{125}Te and ^{123}Te satellites: $\delta(F_A)$, −42.5 ppm; $\delta(F_B)$, −42.1 ppm; $^2J(^{19}F_A-^{19}F_B)$, 186 Hz; $^1J(^{19}F_A-^{125}Te)$, 3400 Hz; $^1J(^{19}F_A-^{123}Te)$, 2780 Hz; $^1J(^{19}F_B-^{125}Te)$, 3605 Hz; $^1J(^{19}F_B-^{123}Te)$, 2995 Hz. The AB_4 patterns are assigned to the $Sb(OTeF_5)_6^-$ anion and are very similar to those reported previously for the $N(CH_3)_4^+Sb(OTeF_5)_6^-$ and $N(CH_2CH_3)_4^+Sb(OTeF_5)_6^-$ in CH_3CN solvent, which are severely second order even at 11.744 T.[34] The second-order spectrum arises when the frequency difference between F_A and F_B, $\nu_o\delta_{AB}$, is small compared to $^1J(^{19}F_A-^{19}F_B)$ and requires no further discussion.

Despite their high receptivities and large dynamic chemical shift ranges, the group 15 nuclides ^{75}As, ^{121}Sb, ^{123}Sb, and

(35) Kolditz, L.; Weisz, D.; Calov, U. *Z. Anorg. Allg. Chem.* **1962**, *316*, 261.
(36) Shamir, J.; Rafaeloff, R. *J. Raman Spectrosc.* **1986**, *17*, 459.
(37) Chemouni, E. *J. Inorg. Nucl. Chem.* **1971**, *33*, 2317.
(38) Cusher, D. W.; Hulme, R. *J. Chem. Soc.* **1964**, 4162.
(39) Murchie, M. P.; Passmore, J.; Sutherland, G. W.; Kapoor, R. *J. Chem. Soc., Dalton Trans.* **1992**, 503.

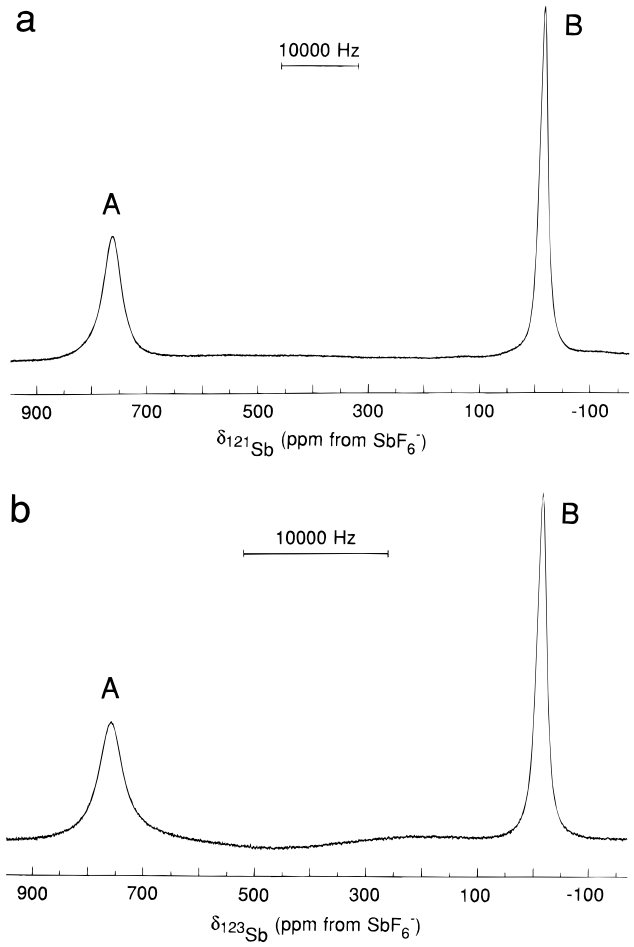

Figure 1. Antimony NMR spectra of $SbCl_4^+Sb(OTeF_5)_6^-$ recorded in SO_2ClF at 27 °C showing (A) $SbCl_4^+$ and (B) $Sb(OTeF_5)_6^-$: (a) ^{121}Sb (71.830 MHz) spectrum; (b) ^{123}Sb (38.899 MHz) spectrum.

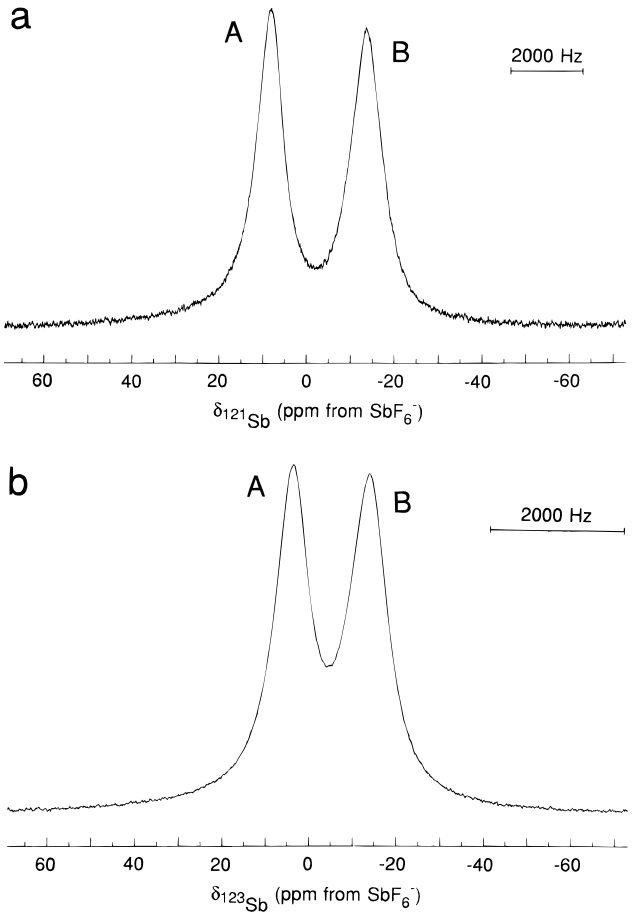

Figure 2. Antimony NMR spectra of $SbBr_4^+Sb(OTeF_5)_6^-$ recorded in SO_2ClF at 27 °C showing (A) $SbBr_4^+$ and (B) $Sb(OTeF_5)_6^-$: (a) ^{121}Sb (119.696 MHz) spectrum; (b) ^{123}Sb (64.820 MHz) spectrum.

^{209}Bi have been little exploited for chemical studies because their quadrupolar nature tends to produce extremely broad resonances, owing to the efficient quadrupolar mechanism which dominates their relaxation behavior. A few NMR studies in which ^{75}As,[34,40−44] ^{121}Sb,[34,40,45−48] ^{123}Sb,[34,47,49] and ^{209}Bi[34,50] nuclides have been employed clearly demonstrate their usefulness, under specific conditions, for structural characterization in solution. A number of these studies are concerned with pnicogen(V) hexahaloanions,[40,45−48,50] but no tetrahalocation of a heavy pnicogen has been characterized by NMR spectroscopy.

The relaxation of a quadrupolar nucleus, under conditions of extreme narrowing, is described by eq 4, where $\Delta\nu_{1/2}$ is the

$$\Delta\nu_{1/2} = \frac{1}{\pi T_2} = \frac{1}{\pi T_1} = \frac{3\pi}{10}\left(\frac{2I+3}{I^2(2I-1)}\right)\left(\frac{e^2qQ}{h}\right)^2\left(1+\frac{\eta^2}{3}\right)\tau_c \quad (4)$$

line width at half-height, T_2 is the spin-spin relaxation time, T_1 is the spin-lattice relaxation time, I is the nuclear spin quantum number, e is the charge on the electron, Q is the nuclear quadrupole moment, q is the electric field gradient (EFG) along the principle z-axis, η is the asymmetry parameter for the EFG, and τ_c is the rotational correlation time.[51] Inspection of several of the factors in this equation reveals that line widths are dramatically reduced for nuclides having a high value of I or a small Q or both.[52] The merits of ^{121}Sb and ^{123}Sb NMR with respect to these points has been discussed previously.[34,41,42,47,50] Narrow line widths are known to arise from quadrupolar nuclei residing at the center of a highly symmetric ligand environment (e.g., O_h or T_d) for which values of q and η are low.[53] The observation of narrow lines therefore requires the pnicogen atom to be located in an electronic environment such that the EFG and η at the antimony nucleus is near zero, as afforded by the local octahedral symmetry of the $Sb(OTeF_5)_6^-$ anion and the T_d point symmetries of the $SbCl_4^+$ and $SbBr_4^+$ cations. Moreover, τ_c serves to increase $\Delta\nu_{1/2}$ of the quadrupolar pnicogen with increasing ionic/molecular radius, increased ion pairing and increasing solvent viscosity (decreasing temperature).

(40) Dove, M. F. A.; Sanders, J. C. P.; Jones, E. L.; Parkin, M. *J. Chem. Soc., Chem. Commun.* **1984**, 1578.
(41) Collins, M. J.; Rao, U. R. K.; Schrobilgen, G. J. *J. Magn. Reson.* **1985**, *61*, 137.
(42) Collins, M. J.; Schrobilgen, G. J. *Inorg. Chem.* **1985**, *24*, 2608.
(43) Balimann, G.; Pregosin, P. S. *J. Magn. Reson.* **1977**, *26*, 283.
(44) McGarvey, G. B.; Moffat, J. B. *J. Magn. Reson.* **1990**, *88*, 305.
(45) Kidd, R. G.; Spinney, H. G. *Can. J. Chem.* **1981**, *59*, 2940.
(46) Goetz-Grandmont, G. J.; Leroy, M. J. F. *Z. Anorg. Allg. Chem.* **1983**, *496*, 40.
(47) Dove, M. F. A.; Sanders, J. C. P. *J. Chem. Soc. Dalton Trans.* **1992**, 3311.
(48) Kidd, R. G.; Matthews, R. W. *J. Inorg. Nucl. Chem.* **1975**, *37*, 661.
(49) (a) Hatton, J. V.; Saito, Y.; Schneider, W. G. *Can. J. Chem.* **1965**, *43*, 47. (b) Dharmatti, S. S.; Weaver, H. E. *Phys. Rev.* **1952**, *87*, 675. (c) Proctor, W. G.; Yu, F. C. *Phys. Rev.* **1951**, *81*, 20. Cohen, V. W.; Knight, W. D.; Wentink, T. *Phys. Rev.* **1950**, *79*, 191.
(50) Morgan, K.; Sayer, B. G.; Schrobilgen, G. J. *J. Magn. Reson.* **1983**, *52*, 139.
(51) Abragam, A. *The Principles of Nuclear Magnetism*; Oxford University Press: London, 1978; Chapter 8.
(52) Sanders, J. C. P.; Schrobilgen, G. J. In *Multinuclear Magnetic Resonance in Liquids and Solids—Chemical Applications*; Granger, P., Harris, R. K., Eds.; NATO ASI Series C; Kluwer Academic Publishers: Boston, MA, 1990; p 157.
(53) (a) Akitt, J. W.; McDonald, W. S. *J. Magn. Reson.* **1984**, *58*, 401. (b) Akitt, J. W. *Prog. NMR Spectrosc.* **1989**, *21*, 401.

The ^{121}Sb and ^{123}Sb NMR spectra of the SbX_4^+ salts obtained in SO_2ClF solvent each consist of two broad singlets (Figures 1 and 2). A peak at −13.6 ppm, common to the spectra of both salts, was assigned to the $Sb(OTeF_5)_6^-$ anion, in good agreement with the previously reported value.[34] Tellurium satellites on the $Sb(OTeF_5)_6^-$ anion spectrum, arising from the two-bond coupling between the ^{121}Sb and ^{123}Sb nuclei and natural abundance ^{125}Te, could not be resolved although they were observed in the $N(CH_3)_4^+$ and $N(CH_2CH_3)_4^+$ salts in the lower viscosity solvent, CH_3CN.[34] The added line broadening may be attributed to the increased viscosity of SO_2ClF, which increases τ_c, and/or ion pairing interactions with the strongly Lewis acidic SbX_4^+ cations, which induce electric field gradients at the antimony nucleus.

The antimony chemical shift of the $SbCl_4^+$ cation (759.9 ppm) is considerably deshielded relative to that of the $SbBr_4^+$ cation (6.3 ppm). The antimony resonances are significantly quadrupole broadened and, in the case of the $SbBr_4^+$ salt, the $Sb(OTeF_5)_6^-$ anion, and the more deshielded $SbBr_4^+$ cation resonances partially overlap in both the ^{121}Sb and ^{123}Sb spectra (Figure 2). Although the larger radius of the $SbBr_4^+$ cation should result in a longer τ_c and larger $\Delta\nu_{1/2}$ values than for $SbCl_4^+$, the opposite effect is found (Table 1) and is attributed to the greater Lewis acidity of the $SbCl_4^+$ cation, which is expected to form a stronger, albeit weak, donor−acceptor bond than $SbBr_4^+$ with the very weakly basic SO_2ClF solvent. An equilibrium concentration of the adduct leads to an increase in the EFG at the antimony nucleus and increased τ_c, which both serve to decrease the relaxation time and increase $\Delta\nu_{1/2}$. The dominance of the quadrupolar relaxation mechanism is confirmed by considering the ratio $\Delta\nu_{1/2}(^{121}\text{Sb})/\Delta\nu_{1/2}(^{123}\text{Sb})$, which is approximately equal to the ratio of the squares of the quadrupole moments (Q) multiplied by the ratio of the spin factors [$f_I = (2I + 3)/(I^2(2I - 1))$] as shown in eq 5. When the

$$\frac{\Delta\nu_{1/2}(^{121}\text{Sb})}{\Delta\nu_{1/2}(^{123}\text{Sb})} \approx \left(\frac{f_I(^{121}\text{Sb})}{f_I(^{123}\text{Sb})}\right)\left(\frac{Q^2(^{121}\text{Sb})}{Q^2(^{123}\text{Sb})}\right) \qquad (5)$$

values of $f_I(^{123}\text{Sb})$ and $f_I(^{121}\text{Sb})$ and the quadrupole moments [$Q(^{121}\text{Sb}) = -0.36(4) \times 10^{-28}$ m^2; $Q(^{123}\text{Sb}) = -0.49(5) \times 10^{-28}$ m^2][54] are substituted into eq 5, the ratio $T_1(^{123}\text{Sb})/T_1(^{121}\text{Sb})$ is found to be 1.27(11). The experimentally determined $\Delta\nu_{1/2}(^{121}\text{Sb})$ and $\Delta\nu_{1/2}(^{123}\text{Sb})$ values for the SbX_4^+ cations and $Sb(OTeF_5)_6^-$ anion give ratios which are in reasonable agreement with the theoretical value and account for the relative broadness of the ^{121}Sb resonances (Table 1). Even though the ^{121}Sb line width is theoretically greater than the ^{123}Sb line width by a factor of 1.27(11), the ^{121}Sb spectra are better resolved and is attributed to a smaller degree of overlap as a result of the higher absolute frequency of ^{121}Sb [$\Xi(^{121}\text{Sb}) = 24.088$ MHz and $\Xi(^{123}\text{Sb}) = 13.047$ MHz for 1 M $SbCl_6^-$ in CH_3CN].[55] This provides a frequency dispersion between the $SbBr_4^+$ and $Sb(OTeF_5)_6^-$ resonances in the ^{121}Sb spectrum which is 1.85 times greater than in the ^{123}Sb spectrum.

An interesting feature relating to the antimony chemical shifts of $SbBr_4^+$ is that the shieldings of $^{121}SbBr_4^+$ and $^{123}SbBr_4^+$ differ by a significant amount (4.8 ppm) even though the ^{121}Sb and ^{123}Sb spectra of $SbBr_4^+Sb(OTeF_5)_6^-$ were recorded on the same sample at the same temperature. Moreover, both chemical shifts are independent of the external field, B_o. The effect is not presently understood, but may, in part, result from relative primary isotopic effects on the NMR shieldings of the antimony nuclei.[56]

Dissolution of $SbBr_4^+Sb(OTeF_5)_6^-$ in CH_3CN near the freezing point of the solvent results in rapid decomposition (see **Syntheses of $SbCl_4^+Sb(OTeF_5)_6^-$ and $SbBr_4^+Sb(OTeF_5)_6^-$**) and contrasts with $SbCl_4^+Sb(OTeF_5)_6^-$, which is stable in CH_3CN solvent at room temperature. Both systems exhibit well-resolved ^{125}Te satellites on the ^{121}Sb and ^{123}Sb NMR spectra of the $Sb(OTeF_5)_6^-$ anions [$^2J(^{121}\text{Sb}-^{125}\text{Te})$, 752 Hz; $^2J(^{123}\text{Sb}-^{125}\text{Te})$, 407 Hz]. No antimony resonance attributable to the $SbBr_2^+$ cation is expected because of its low symmetry. In the case of $SbCl_4^+$, a very broad resonance centered at ca. 660 ppm [$\Delta\nu_{1/2}(^{121}\text{Sb})$, 20 500 Hz] was observed in CH_3CN and is attributed to solvated $SbCl_4^+$. The chemical shift of the complex cation is expected to be more shielded than that of $SbCl_4^+$ in SO_2ClF solution and broadened by the resultant large EFG at the antimony nucleus in a five-coordinate 1:1 adduct or six-coordinate 1:2 *cis*- or *trans*-adduct.

According to the formalism developed by Jameson and Gutowsky,[57] the large variation in Sb shielding arises from the dominant and negative paramagnetic shielding term, σ_p. The magnitude of σ_p is directly proportional to changes in the inverse mean excitation energy (ΔE^{-1}), the mean inverse cubes of the p and d electron−nucleus distances ($\langle r^{-3}\rangle_{np}$ and $\langle r^{-3}\rangle_{nd}$) and the valence imbalance in the p and d orbitals centered on the Sb atom (P_i and D_i). The relative chemical shifts of the SbX_4^+ and SbX_6^- ions follow the valence imbalance terms and are dependent upon the electron density and the relative electronegativities of the halogens. The electronegativity difference of chlorine and bromine qualitatively accounts for the high-frequency shifts of $SbCl_4^+$ (759.9 ppm) and $SbCl_6^-$ (−86.7 ppm)[47] relative to those of $SbBr_4^+$ (6.3 ppm) and $SbBr_6^-$ (−2517 ppm),[45] and the formal positive charge, which is expected to reside mainly on the Sb atom, accounts for the high-frequency shift of the SbX_4^+ cations compared to the SbX_6^- anions, which have their formal negative charge located on the halogens. Interestingly, the chemical shift difference between $SbBr_4^+$ and $SbBr_6^-$ is much larger (2523 ppm) than between $SbCl_4^+$ and $SbCl_6^-$ (845 ppm). The $SbBr_4^+$ and $SbBr_6^-$ ions are both yellow whereas the $SbCl_4^+$ and $SbCl_6^-$ ions are colorless. The LUMO's are expected to be lower in the bromine ions so that their respective first allowed optical transitions can be expected to move to longer wavelengths and into the visible spectrum. A relative decrease in the HOMO−LUMO separation increases the ΔE^{-1} term and could account for the greater paramagnetic deshielding of the bromine ions relative to each other.

The ^{121}Sb and ^{123}Sb chemical shifts obtained in this work, together with previously reported ^{121}Sb and ^{123}Sb shifts, may be compared with known values of corresponding phosphorus(V) and arsenic(V) compounds when the ^{31}P and ^{75}As chemical shifts are also referenced to the hexafluoropnictate anions, PnF_6^-. A larger dynamic chemical shift range is anticipated for the heavier pnicogen analogs as a result of their larger $\langle r^{-3}\rangle_{np}$ and $\langle r^{-3}\rangle_{nd}$ values. This expectation is not always met. The chemical shift of the $SbCl_4^+$ cation (759.9 ppm) is larger than that of PCl_4^+ (218 to 241 ppm),[58] whereas the shifts of the

(54) Mills, I.; *et al*. *Quantities, Units and Symbols in Physical Chemistry*, 2nd ed.; Blackwells: Oxford, England, 1993.
(55) *Multinuclear NMR*; Mason, J., Ed.; Plenum Press: New York, 1987; Appendix, p 627.
(56) Jameson, C. J.; Mason, J. In *Multinuclear NMR*; Mason, J., Ed.; Plenum Press: New York, **1987**; Chapter 3, pp 80−82.
(57) Jameson, C. J.; Gutowsky, H. S. *J. Chem. Phys.* **1964**, *40*, 1714.
(58) (a) Hudson, H. R.; Dillon, K. B.; Walker, B. J. In *CRC Handbook of Phosphorus-31 Nuclear Magnetic Resonance Data*; Tebby, J. C., Ed.; CRC Press: Boston, MA, 1991; Chapter 8, pp 181−221 and references therein. (b) Lamandé, L.; Koenig, M.; Dillon, K. B. *ibid*.; Chapter 19, pp 553−565 and references therein.

Table 2. Summary of Crystal Data and Refinement Results for $SbCl_4^+Sb(OTeF_5)_6^-$ and $SbBr_4^+Sb(OTeF_5)_6^-$

chem formula	$Cl_4F_{30}O_6Sb_2Te_6$	$Br_4F_{30}O_6Sb_2Te_6$
space group	$P\bar{3}$	$P\bar{3}$
a (Å)	10.022(1)	10.206(1)
c (Å)	18.995(4)	19.297(3)
V (Å^3)	1652.3(6)	1740.9(5)
molecules/unit cell	2	2
mol wt	1816.90	1994.74
calcd density (g cm^{-3})	3.652	3.806
T (°C)	−75	−81
μ (cm^{-1})	38.7	59.8
λ (Å)	0.560 86	0.560 86
R_1[a]	0.0461	0.0425
wR_2[b]	0.1223	0.1014

[a] R_1 is defined as $\sum||F_o| - |F_c||/\sum|F_o|$. [b] wR_2 is defined as $[\sum[w(F_o^2 - F_c^2)^2]/\sum w(F_o^2)^2]^{1/2}$.

$PnBr_4^+$ cations show the reverse order ($SbBr_4^+$, 3.9 to 8.6 ppm; PBr_4^+, 65 to 79 ppm).[58] The shielding order among the hexachloroanions of the three pnicogens P, As, and Sb is also unusual. The Sb nucleus in $SbCl_6^-$ is less shielded (−87.6 ppm) than the pnicogen nucleus in either PCl_6^- (−152 ppm)[59] or $AsCl_6^-$ (−392 ppm)[40] and has been noted previously.[34,47] Comparable behavior has also been noted for the $As(OTeF_5)_6^-$ and $Sb(OTeF_5)_6^-$ anions, where the Sb nucleus (−13.8 ppm) is less shielded than the As nucleus (−29.1 ppm).[34] In both cases, the negative chemical shift is in agreement with the $OTeF_5$ group being less electronegative than F, but the ^{209}Bi resonance in $Bi(OTeF_5)_6^-$ (126.7 ppm) occurs to higher frequency of the BiF_6^- reference standard.[34] The reasons for their apparent anomalous behavior are not understood, since the number of known ^{75}As, ^{121}Sb, ^{123}Sb, and ^{209}Bi chemical shifts is still very limited, but it may, in part, be a consequence of significant relativistic effects on the Sb and Bi atoms.[60,61]

X-ray Crystal Structures of $SbCl_4^+Sb(OTeF_5)_6^-$ and $SbBr_4^+Sb(OTeF_5)_6^-$. Details of the data collection parameters and other crystallographic information for the $P\bar{3}$ space group are given in Table 2. The final atomic coordinates and the equivalent isotropic thermal parameters are summarized in Table 3. Important bond lengths and angles for the $SbCl_4^+$ and $SbBr_4^+$ cations, together with bond lengths and angles for the $Sb(OTeF_5)_6^-$ anions are listed in Table 4 and Supporting Information Table 11. The bond valences for individual bonds in the two cations and for their long contacts as defined by Brown[63] are also included in Table 4. While the $SbBr_4^+$ cation and its structure are reported for the first time in the present paper, the structure of the $SbCl_4^+$ cation has been reported previously, but its structural parameters are more accurately determined in the present structure (*vide infra*).[64]

Both compounds exhibit merohedral twinning with twin laws $m \perp [001]$ (see **Experimental Section**) and display the same crystallographic features. The compounds consist of well-separated SbX_4^+ (X = Cl and Br) cations and $Sb(OTeF_5)_6^-$ anions (Figure 3). In these and the previously reported $N(CH_3)_4^+$ and $N(CH_2CH_3)_4^+$ salts[34] of the $Sb(OTeF_5)_6^-$ anion that have been crystallographically characterized, the central antimony atom is bonded octahedrally to the six oxygen atoms and each of the six tellurium atoms is octahedrally bonded to an oxygen and five fluorines so that each anion can be described as an octahedron of octahedra. In the present structures, the central antimony atoms lie on inversion centers, so that the anions have $\bar{3}$ symmetry imposed on them by their lattices. While both SbX_4^+ cations are perfectly ordered and have the expected tetrahedral geometry, one of the two crystallographically independent anions is perfectly ordered and the other suffers from an orientational disorder (Figure 3). This disorder only affects the light atoms and can be described as the superposition of two anions where the Sb and Te atoms occupy the same positions; their respective thermal parameters are as low as those observed in the non- disordered anions (Table 3). The two orientations could be easily resolved for all the oxygen and fluorine atoms and were found to differ by 15° in the $SbCl_4^+$ salt and by 22° in the $SbBr_4^+$ salt (see **Experimental Section**).

The bond lengths and bond angles of the $Sb(OTeF_5)_6^-$ anions in the $SbCl_4^+$ salt (denoted in parentheses) and the $SbBr_4^+$ salt

Table 3. Atomic Coordinates ($\times 10^4$) and Equivalent Isotropic Displacement Parameters (Å^2 $\times$ 10^3) for $SbCl_4^+Sb(OTeF_5)_6^-$ and $SbBr_4^+Sb(OTeF_5)_6^-$

	x	y	z	U(eq)[a]
		$SbCl_4^+Sb(OTeF_5)_6^-$		
Sb(1)	6667	3333	7123(1)	27(1)
Cl(1)	8832(2)	3535(3)	7537(1)	35(1)
Cl(2)	6667	3333	5953(2)	39(1)
Sb(2)	0	10000	5000	14(1)
O(1)	49(6)	8430(6)	5586(3)	21(1)
Te(1)	1405(1)	8197(1)	6149(1)	21(1)
F(1)	3140(6)	9816 (7)	5780(3)	34(1)
F(2)	1373(7)	9491(7)	6815(3)	33(1)
F(3)	−229(8)	6549(7)	6558(3)	41(1)
F(4)	1573(8)	6898(8)	5533(4)	43(2)
F(5)	2639(8)	7875(7)	6739(4)	42(1)
Sb(3)	0	0	0	20(1)
Te(2)	−2453(1)	−3238(1)	1072(1)	36(1)
O(2)	−1718(16)	−1429(16)	579(11)	67(4)
F(6)	−3117(29)	−4213(26)	229(7)	77(2)
F(7)	−724(18)	−3396(30)	1056(14)	77(2)
F(8)	−1828(29)	−1781(21)	1761(9)	77(2)
F(9)	−4226(17)	−3160(29)	1170(13)	77(2)
F(10)	−3521(26)	−5071(15)	1533(12)	77(2)
O(3)	−1819(9)	−1779(18)	374(9)	67(4)
F(11)	−3133(30)	−4633(23)	359(9)	77(2)
F(12)	−686(19)	−3235(33)	1295(14)	77(2)
F(13)	−2082(32)	−2228(26)	1908(7)	77(2)
F(14)	−4366(15)	−3459(31)	962(14)	77(2)
F(15)	−3279(30)	−4753(21)	1735(10)	77(2)
		$SbBr_4^+Sb(OTeF_5)_6^-$		
Sb(1)	1333	6667	2871(1)	26(1)
Br(1)	11033(1)	4622(1)	2437(1)	37(1)
Br(2)	13333	6667	4110(1)	40(1)
Sb(2)	10000	0	5000	18(1)
O(1)	8427(6)	19(6)	4432(3)	25(1)
Te(1)	8145(1)	1304(1)	3870(1)	25(1)
F(1)	6843(9)	1400(9)	4484(4)	55(2)
F(2)	9707(7)	3051(6)	4234(4)	43(1)
F(3)	9446(7)	1325(7)	3211(3)	38(1)
F(4)	6557(7)	−352(7)	3461(4)	49(2)
F(5)	7776(7)	2487(7)	3289(4)	49(2)
Sb(3)	10000	0	0	21(1)
Te(2)	7619(1)	838(1)	1043(1)	38(1)
O(2)	8521(18)	−173(15)	686(7)	63(4)
F(6)	5734(10)	−827(14)	954(11)	77(2)
F(7)	7718(22)	34(21)	1873(5)	77(2)
F(8)	9413(12)	2553(13)	1216(11)	77(2)
F(9)	6991(21)	1105(21)	198(5)	77(2)
F(10)	6537(19)	1629(21)	1434(9)	77(2)
O(3)	8207(10)	−41(18)	377(8)	63(4)
F(11)	6016(15)	−1025(12)	1236(11)	77(2)
F(12)	8473(20)	389(24)	1768(7)	77(2)
F(13)	9205(16)	2748(11)	905(11)	77(2)
F(14)	7012(25)	1705(22)	389(8)	77(2)
F(15)	6853(23)	1498(24)	1729(7)	77(2)

[a] U(eq) is defined as one-third of the trace of the orthogonalized $\mathbf{U}_{ij}$ tensor.

(59) Il'in, E. G.; Shcherbakova, M. N.; Buslaev, Y. A. *Koord. Khim.* **1975**, *1*, 1179.
(60) Pyykkö, P. *Chem. Rev.* **1988**, *88*, 563 and references therein.
(61) Pyykkö, P.; Wiesenfeld, L. *Mol. Phys.* **1981**, *43*, 557.
(62) Brese, N. E.; O'Keeffe, M. *Acta Crystallogr.* **1991**, *B47*, 192.
(63) Brown, I. D. *J. Solid State Chem.* **1974**, *11*, 214.

Table 4. Bond Lengths (Å), Bond Valences (vu) and Bond Angles (deg) in $SbCl_4^+Sb(OTeF_5)_6^-$ and $SbBr_4^+Sb(OTeF_5)_6^-$

	$SbCl_4^+$		
	Cl(1)	Cl(2)	F(3)
Sb(1)	2.221(2)	2.222(4)	3.346(2)
bv[a]	1.238	1.235	0.015
total	4.994		
Cl(1)−Sb(1)−Cl(1A)		108.14(8)	
Cl(1)−Sb(1)−Cl(2)		110.78(8)	
	$SbBr_4^+$		
	Br(1)	Br(2)	F(4)
Sb(1)	2.381(1)	2.391(2)	3.372(1)
bv[a]	1.238	1.205	0.014
total	4.961		
Br(1)−Sb(1)−Br(1A)		108.31(4)	
Br(1)−Sb(1)−Br(2)		110.62(4)	

	$SbCl_4^+Sb(OTeF_5)_6^-$	$SbBr_4^+Sb(OTeF_5)_6^-$
Sb(2)−O(1)	1.947(5)	1.952(5)
Sb(3)−O(2)	1.938(4)	1.949(5)
Sb(3)−O(3)	1.938(4)	1.950(5)
mean Te−O	1.835(4)	1.831(5)
mean Te−F	1.825(5)	1.826(5)
Sb(2)−O(1)−Te(1)	139.1(3)	139.8(3)
Sb(3)−O(2)−Te(2)	142.1(5)	142.3(6)
Sb(3)−O(3)−Te(2)	142.1(5)	141.7(6)

[a] Bond valence units (vu) are defined in ref 63. $R_o = 2.30$ (Sb−Cl), $R_o = 1.80$ (Sb−F), $R_o = 2.46$ (Sb−Br), and $B = 0.37$ were used.

(denoted in square brackets) are equal within experimental error and are discussed together. The Sb−O distances Sb(2)−O(1) (1.947(5) [1.952(5)] Å) and Sb(3)−O(2)/O(3) (1.938(4)/1.938(4) [1.949(5)/1.950(5)] Å) are comparable to the average librationally corrected Sb^V−O distances observed in $N(CH_3)_4^+Sb(OTeF_5)_6^-$ and $N(CH_2CH_3)_4^+Sb(OTeF_5)_6^-$ (1.96 and 1.91 Å, respectively),[34] $Cs_3Sb_3F_{12}O_3$ (1.92 Å),[65] and $Rb_2(Sb_2F_{10}O)$ (1.91 Å),[66] where the Sb atoms are also octahedrally coordinated to bridging oxygen atoms. The Te−O (1.835(4) [1.831(5)] Å) and the average Te−F (1.825(5) [1.826(5)] Å) bond distances (Table 4), are comparable to those found in many other $OTeF_5$ compounds.[34,67,68] The Sb−O−Te angles reported here (Sb(2)−O(1)−Te(1) = 139.1(3)° [139.8(3)°]; Sb(3)−O(2)/O(3)−Te(2) = 142.1(5)/142.1(5)° [142.3(6)/141.7(6)°]), differ from those reported previously for $N(CH_3)_4^+Sb(OTeF_5)_6^-$ (148.4(8)−153.4(8)°) and $N(CH_2CH_3)_4^+Sb(OTeF_5)_6^-$ (160.7(9)−167(1)°), but are identical to those reported for $N(CH_3)_4^+As(OTeF_5)_6^-$ (139.9(6)−141(2)°, $R\bar{3}$ space group).[34] This result confirms that the M−O−Te angles are not solely dependent on the nature of the M atom or the counter cation, but are largely dependent on the crystal packing.[34]

Despite the fact that the four halogen atoms are not symmetry related, with one of the halogen atoms of each cation positioned on a C_3-axis and the other three halogen atoms on general positions, the four Sb^V−X bond lengths of both cations are identical within 3σ [Sb−Cl, 2.221(2) × 3 and 2.222(4) × 1 Å; Sb−Br,

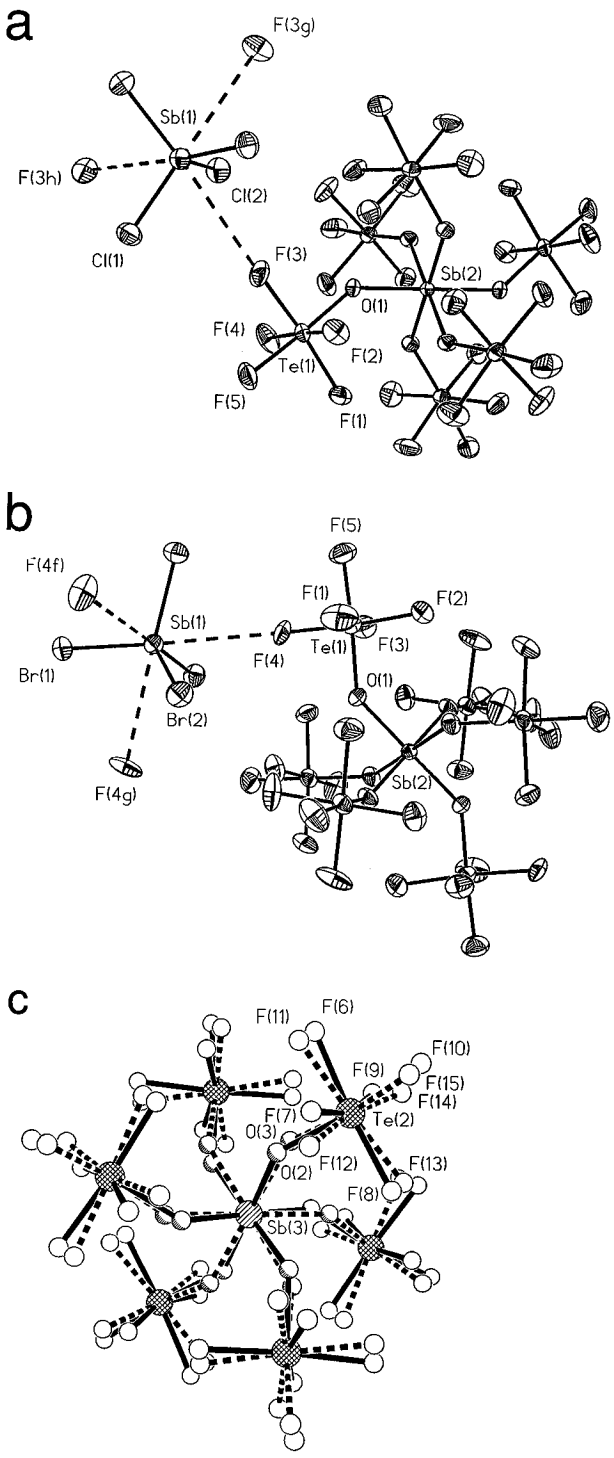

Figure 3. Geometries of (a) the $SbCl_4^+$ cation and ordered $Sb(OTeF_5)_6^-$ anion and (b) the $SbBr_4^+$ cation and ordered $Sb(OTeF_5)_6^-$ anion. In both cases the coordination environment of the SbX_4^+ cations with fluorine atoms of three different anions are denoted by dashed lines. Thermal ellipsoids are shown at the 50% probability level. (c) Geometry of the disordered $Sb(OTeF_5)_6^-$ anion in $SbBr_4^+Sb(OTeF_5)_6^-$. The two orientations are 22° apart and 15° apart in the $SbCl_4^+$ analog (not shown).

(64) The structure of $SbCl_4^+Sb_2Cl_2F_9^-$ was refined to a final residual of 0.14,[20] and the structure of $SbCl_4^+Sb_2F_{11}^-$ has only been published in a preliminary communication and was never refined beyond $R = 0.19$.[21] In the course of an extensive investigation of the structures of mixed antimony(V) chloride fluorides, the crystal structure of $SbCl_4^+Sb_2Cl_2F_9^-$ was claimed to have been reexamined,[23] but only the lattice constants were redetermined (Ballard, J. G. Ph.D. Thesis, McMaster University, 1977) and ^{121}Sb Mössbauer spectra reported (Birchall, T.; Ballard, J. G. *J. Phys. Paris* **1976**, *37*, C6-513). No subsequent attempts have been made to obtain a more precise solution of the structure. The structure of $SbCl_4^+Sb_2Cl_{0.5}F_{10.5}^-$ has been refined to a residual of 0.054,[22] but the solution of the structure was based on the atomic coordinates of the ill-defined $SbCl_4^+Sb_2Cl_2F_9^-$ salt. Moreover, in the "$Sb_2Cl_{0.5}F_{10.5}^-$" anion, two ligand positions are statistically occupied by Cl and F, leading to an average stoichiometry, suggesting the presence of more than one anion type.

(65) Haase, W. *Acta Crystallogr.* **1974**, *B30*, 2465.
(66) Haase, W. *Acta Crystallogr.* **1974**, *B30*, 2508.
(67) Lentz, D.; Pritzkow, H.; Seppelt, K. *Inorg. Chem.* **1978**, *17*, 1926.
(68) Sawyer, J. F.; Schrobilgen, G. J. *Acta Crystallogr.* **1982**, *B38*, 1561.

2.381(1) × 3 and 2.391(2) × 1 Å], and the average angles are close to the ideal tetrahedral value [Cl(1)−Sb(1)−Cl(1), 108.14(8)°; Cl(1)−Sb(1)−Cl(2), 110.78(8)°; Br(1)−Sb(1)−Br(1), 108.31(4)°; Br(1)−Sb(1)−Br(2), 110.62(4)°]. To our knowledge, the present $Sb^{V}-X$ bond lengths are the shortest and least polar Sb−X bonds known, being shorter than in the $Sb^{V}X_6^-$ anions (Cl, 2.357(4) Å;[69] Br, 2.546(11),[70a] 2.565(5),[70b] 2.563(6)[70c] Å) and the $Sb^{III}-X$ bond lengths in the neutral $Sb^{III}X_3$ (Cl, 2.37(2),[71a] 2.36(3),[71b] 2.359(3)[71c] Å; Br, 2.49(2),[72] 2.50(3)[37] Å), the $Sb^{III}X_4^-$ (Cl, 2.365(3) Å;[73] Br, 2.564(3) Å[74]), $Sb^{III}X_5^{2-}$ (Cl, 2.385(2) (ax) and 2.623(2) (eq) Å;[75] Br, 2.580(5) (ax) and 2.787(7) (eq) Å[76]) and $Sb^{III}X_6^{3-}$ (Cl, 2.652(6) Å;[77] Br, 2.799(7),[70a] 2.795(6)[70c] Å) anions. The $Sb^{V}-X$ bond lengths are also shorter and less polar than the Sn−X, In−X and Cd−Br bond lengths observed in the isoelectronic neutral molecules SnX_4 (Cl, 2.280 Å;[78] Br, 2.40(3) Å[79]) and anions InX_4^- (Cl, 2.350(3) Å;[80] Br, 2.479(3),[80] 2.489(3)[81] Å) and $CdBr_4^{2-}$ (2.560 Å[82]). The Sb−X bond lengths fit series in which the PnX_4^+ bond lengths increase monotonically with the mass of the pnicogen: NCl_4^+ (1.764 Å)[83] < PCl_4^+ (1.927(2) Å)[12] < $AsCl_4^+$ (2.0545(9) Å)[4] < $SbCl_4^+$ (2.221(2) Å)[84] and PBr_4^+ (2.17(1) Å)[13] < $AsBr_4^+$ (2.221 Å)[85] < $SbBr_4^+$ (2.385(2) Å).[84]

The structural parameters of the $SbCl_4^+$ cation, though better determined in the $Sb(OTeF_5)_6^-$ salt, are in agreement with those previously reported (Sb−Cl bond lengths and Cl−Sb−Cl bond angle: in the $Sb_2F_{11}^-$ salt, 2.22(3) Å;[21] $Sb_2Cl_{0.5}F_{10.5}^-$, 2.21(1) Å and 107(1)−114(1)°;[22] $Sb_2Cl_2F_9^-$, 2.16(3)−2.20(3) Å and 107(2)−117(2)° [20]). In $SbCl_4^+Sb(OTeF_5)_6^-$, each cation has three long Sb(1)···F contacts with three fluorine atoms belonging to three different ordered Sb(2) anions ($SbCl_4^+$: Sb(1)···F(3), 3.346(2) × 3 Å) which pass through the centers of three of the faces of the tetrahedron (those containing the halogen atom positioned on the C_3-axis (Cl(1)), whereas the face containing the three symmetry-related halogen atoms (Cl(2)) does not have any long Sb(1)···F contacts (Figure 3). In the three previously reported structures, the $SbCl_4^+$ cation has four long Sb···F long contacts, each passing through the center of one of the four faces of the tetrahedron, with the four fluorine atoms forming a tetrahedron around the $SbCl_4^+$ cation ($Sb_2F_{11}^-$, 3.0 Å;[21] $Sb_2Cl_{0.5}F_{10.5}^-$, 2.98(2)−3.35(2) Å;[22] $Sb_2Cl_2F_9^-$, 2.926−3.259 Å[20]). Three analogous long Sb(1)···F contacts are observed in $SbBr_4^+Sb(OTeF_5)_6^-$ (Sb(1)···F(4), 3.372(1) × 3 Å). Although the Sb(1)···F distances to $SbCl_4^+$ and $SbBr_4^+$ are smaller than the sum of the van der Waals radii (3.55[86] −3.60[87] Å), bond valence calculations suggest that the Sb(1)···F interactions are weak interactions, i.e., the total bond valence for each antimony atom is 4.994 [4.962] vu (bond valence units), with contributions of 1.238−1.235 [1.238−1.205] vu/Cl [Br] atom and 0.015 [0.014] vu/long fluorine contact. In comparison with the three anions that have been previously used to stabilize the $SbCl_4^+$ cation, the $Sb(OTeF_5)_6^-$ anion is the weakest coordinating anion. This is reflected in the smaller number of long anion−cation contacts and in longer Sb···F contacts than observed in previous $SbCl_4^+$ structures.[20−22] The occurrence of long contacts between the central atom of the cation and fluorines of the anion is a feature also encountered in $AsCl_4^+AsF_6^-$.[4] The As atom has four long As···F contacts at 3.345 Å which is at the limit of the sum of the van der Waals radii for arsenic and fluorine (3.35[86]−3.40[87] Å). The contacting fluorines are symmetrically disposed about the $AsCl_4^+$ cation in a tetrahedral arrangement analogous to those observed in $Sb_2F_{11}^-$, $Sb_2Cl_{0.5}F_{10.5}^-$ and $Sb_2Cl_2F_9^-$.

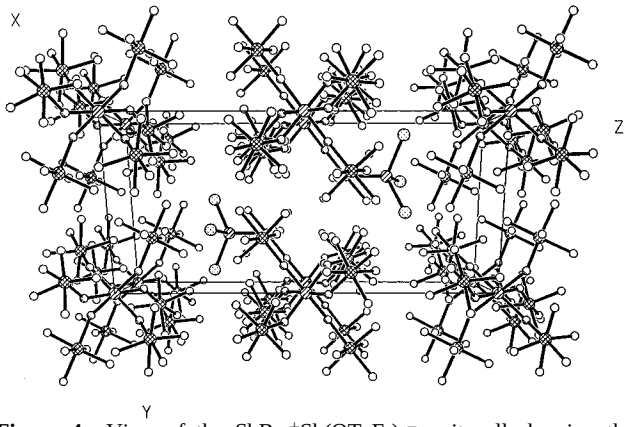

Figure 4. View of the $SbBr_4^+Sb(OTeF_5)_6^-$ unit cell showing the packing along the *x*-axis. For clarity, the F atoms have been omitted.

Other anion−cation contacts occur between the halogen atoms, and several fluorine atoms of both the Sb(2) and Sb(3) anions ($SbCl_4^+$: Cl(1)···F(12), 3.005 × 1, Cl(2)···F(3), 3.370 × 3 and Cl(2)···F(4), 3.396 × 3 Å) ($SbBr_4^+$: Br(1)···F(3), 3.043 × 1, Br(1)···F(8), 3.275 × 1, Br(2)···F(1), 3.411 × 3, and Br(2)···F(4), 3.413 × 3 Å) and are at the limit of the X···F van der Waals distance (3.15[86]−3.20[87] [3.30[86]−3.35[87]]).

The crystal structures of $SbX_4^+Sb(OTeF_5)_6^-$ are dominated by the larger $Sb(OTeF_5)_6^-$ anions and consist of hexagonal closest packed anion lattices with the cations occupying what are formally octahedral interstitial sites but are, in fact, trigonal prismatic holes with three anions from each layer defining the site. The cation/anion radius ratios are found to be greater than the minimum 0.414 value required for octahedral interstitial sites[88] (0.596−0.602 [0.636−0.639]). Interestingly, the SbX_4^+ cations are not located in the middle of the trigonal prismatic hole, but are closer to the layer containing the nondisordered Sb(2) anions (7.183 × 3 Å) than the layer containing the disordered Sb(3) anions (8.088 × 3 Å) (Figure 4). This displacement can be understood by considering the total bond valence around the Sb atom in the SbX_4^+ cations. If the cations were positioned at the centers of the trigonal prismatic sites, the cations would have equal but long Sb(1)···F contacts with the fluorines of both the Sb(2) and Sb(3) anions. The contacts would be too long to contribute to the total bond valence of

(69) Gillespie, R. J.; Sawyer, J. F.; Slim, D. R.; Tyrer, J. D. *Inorg. Chem.* **1982**, *21*, 1296.
(70) (a) Lawton, S. L.; Jacobson, R. A.; Frye, R. S. *Inorg. Chem.* **1971**, *10*, 701. (b) Hackert, M. L.; Jacobson, R. A. *Inorg. Chem.* **1971**, *10*, 1075. (c) Lawton, S. L.; Jacobson, R. A. *Inorg. Chem.* **1966**, *5*, 743.
(71) (a) Allen, P. W.; Sutton, L. E. *Acta Crystallogr.* **1950**, *3*, 46. (b) Lindqvist, I.; Niggli, A. *J. Inorg. Nucl. Chem.* **1956**, *2*, 345. (c) Lipka, A. *Acta Crystallogr.* **1979**, *B35*, 3020.
(72) Cusher, D. W.; Hulme, R. *J. Chem. Soc.* **1962**, 2218.
(73) Porter, S. K.; Jacobson, R. A. *J. Chem. Soc. A* **1970**, 1356.
(74) Dehaven, P. W.; Jacobson, R. A. *Cryst. Struct. Commun.* **1976**, *5*, 393.
(75) Wismer, R. K.; Jacobson, R. A. *Inorg. Chem.* **1974**, *13*, 1678.
(76) Carola, J. M.; Freedman, D. D.; McLaughlin, K. L.; Reim, P. C.; Schmidt, W. J. *Cryst. Struct. Commun.* **1976**, *5*, 393.
(77) Schroeder, D. R.; Jacobson, R. A. *Inorg. Chem.* **1973**, *12*, 210.
(78) *CRC Handbook of Chemistry and Physics*, 75th ed.; Lide, D. R. Ed.; CRC Press: Boca Raton, FL, 1995; pp 9−23.
(79) Brand, P.; Sackmann, H. *Acta Crystallogr.* **1963**, *16*, 446.
(80) Khan, M. A.; Tuck, D. G. *Acta Crystallogr.* **1982**, *B38*, 803.
(81) Beno, M. A.; Cox, D. D.; William, J. M.; Kwak, J. F. *Acta Crystallogr.* **1984**, *C40*, 1334.
(82) Altermatt, D.; Arend, H.; Gramlich, V.; Niggli, A.; Petter, W. *Acta Crystallogr.* **1984**, *B40*, 347.
(83) Sawodny, W.; Hartner, H.; Minkwitz, R.; Bernstein, D. *J. Mol. Struct.* **1989**, *213*, 145.
(84) This work.
(85) This work; see Table 7.
(86) Pauling, L. *The Nature of the Chemical Bond*, 3rd ed.; Cornell University Press: Ithaca, NY, 1960; Chapter 7, p 260.
(87) Bondi, A. *J. Phys. Chem.* **1964**, *68*, 441.
(88) Pauling, L. *The Nature of the Chemical Bond*, 3rd. ed.; Cornell University Press: Ithaca, NY, 1960; Chapter 13, p 545.

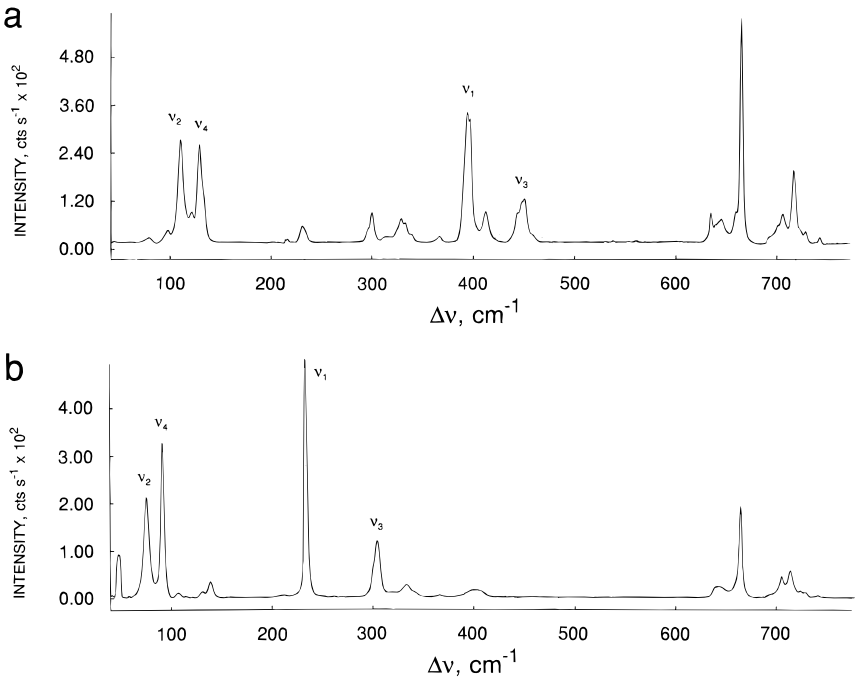

Figure 5. Raman spectra of microcrystalline (a) $SbCl_4^+Sb(OTeF_5)_6^-$ (−150 °C) and (b) $SbBr_4^+Sb(OTeF_5)_6^-$ (−152 °C) recorded using 514.5-nm excitation. $\nu_1-\nu_4$ denote cation bands.

Table 5. Raman Frequencies and Assignments in $SbCl_4^+Sb(OTeF_5)_6^-$ and $SbBr_4^+Sb(OTeF_5)_6^-$ [a]

freq, cm^{-1}		assignments	
$SbCl_4^+Sb(OTeF_5)_6^-$	$SbBr_4^+Sb(OTeF_5)_6^-$	cation	anion[b]
450.7 (19)	304.9 (23)	$\nu_3(T_2)$	
395.6 (60)	234.4 (100)	$\nu_1(A_1)$	
139.4 (45)	92.1 (63)	$\nu_4(T_2)$	
121.5 (47)	76.2 (42)	$\nu_2(E)$	
744 (3)	741 (<1)		$\nu_8(E)$, $\nu_{as}(TeF_4)$
730 (6)	729 (2)		
724 (6)	724 (3)		
718 (34)	715 (11)		$\nu_1(A_1)$, ν(TeF)
708 (14)	706 (9)		
703 (9)			
695(4)	695 (3)		
666 (100)	665 (38)		$\nu_2(A_1)$, $\nu_s(TeF_4)$
661 (11)	660 (4), sh		
646 (8)	644 (4)		$\nu_5(B_1)$, $\nu_{as}(TeF_4)$
636 (12)	640 (6)		
457 (5), sh			$\nu_3(A_1)$, ν(TeO)
412 (14)			coupled with ν_s(Sb−O)
402 (8), sh	402 (4), br		
368 (3)	366 (2)		*c*
342 (4)	342 (1), sh		$\nu_9(E)$, $\delta(FTeF_4)$
336 (9)	334 (4)		
332 (11)			
316 (3)			$\nu_{10}(E)$, $\delta(OTeF_5)$
304 (13)	305 (24)		$\nu_4(A_1)$, $\delta_s(FTeF_4)$;
300 (6), sh	301 (12), sh		$\nu_7(B_2)$, $\delta_{sciss}(TeF_4)$
238 (8)			$\nu_{11}(E)$, $\delta_{as}(TeF_4)$
223 (2)	211 (<1)		δ(TeOSb)
143 (2), sh	140 (7)		τ(TeOSb)
132 (14)	131 (2)		
109 (6)	107 (2)		lattice modes
91 (4)	50 (18)		

[a] Values in parentheses denote relative intensities and sh denotes a shoulder and br a broad line. [b] The vibrational modes of the $OTeF_5$ groups are assigned under C_{4v} symmetry (see ref 34). [c] Unassigned anion mode.

Sb(1) so that the total bond valence of five for the Sb(1) atom of the cation would not be met. It appears that the Sb(1)···F contacts serve to constrain the Sb(2) anion in one orientation, while the absence of contacts with the fluorines of the Sb(3) anion accounts for the disorder on this anion.

Table 6. Correlation Diagram for the Vibrational Modes of the SbX_4^+ Cations (X = Cl and Br) in $SbX_4^+Sb(OTeF_5)_6^-$

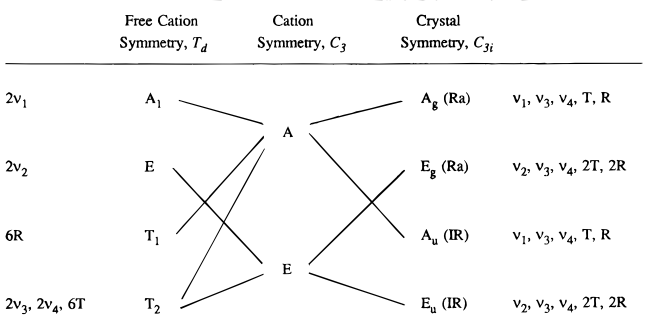

Raman Spectra of $SbCl_4^+Sb(OTeF_5)_6^-$ and $SbBr_4^+Sb(OTeF_5)_6^-$ and the General Valence Force Field (GVFF) Analyses of $SbCl_4^+$, $SbBr_4^+$, and Related Tetrahalocations. The solid-state Raman spectra of the title compounds are shown in Figure 5. The observed frequencies and their assignments are summarized in Table 5. The assignments of the frequencies for the $Sb(OTeF_5)_6^-$ anion were made by comparison with the recent assignments for $N(CH_3)_4^+Sb(OTeF_5)_6^-$,[34] and consequently require no further comment. The vibrational modes of the SbX_4^+ cations were assigned under T_d point symmetry and belong to the irreducible representation $\Gamma = A_1 + E + 2T_2$. A total of four vibrational bands are expected, $\nu_1(A_1)$, $\nu_2(E)$, $\nu_3(T_2)$, $\nu_4(T_2)$, all of which are Raman active while the $\nu_3(T_2)$ and $\nu_4(T_2)$ bands are infrared active. A factor-group analysis correlating the T_d point symmetries of the free SbX_4^+ cations to their crystallographic site symmetries (C_3) and to the symmetry of the unit cell (C_{3i}) is given in Table 6. The analysis reveals that $\nu_1(A_1)$ and $\nu_2(E)$ appear as Raman-active A_g and E_g components, respectively, under the crystal symmetry and are not split, whereas $\nu_3(T_2)$ and $\nu_4(T_2)$ are each split into Raman-active A_g and E_g components which are not, in practice, resolved in the Raman spectrum. The Raman spectra of the $SbCl_4^+$ cation in $SbCl_4^+Sb_2Cl_2F_9^-$ and $SbCl_4^+Sb_2F_{11}^-$ have been reported[20,23] and are in good agreement with the cation frequencies in $SbCl_4^+Sb(OTeF_5)_6^-$. We report here the Raman spectra of $SbCl_4^+$ and $SbBr_4^+$ and the results of normal coordinate

Table 7. Raman Frequencies, General Valence Force Constants, and Bond Lengths for $SbCl_4^+$ and $SbBr_4^+$ and Related Species

	frequency, cm^{-1}					general valence force constants[a]					M−X	
MX_4	$\nu_1(A_1)$	$\nu_2(E)$	$\nu_3(T_2)$	$\nu_4(T_2)$	ref	f_r	f_{rr}	f_α	$f_{\alpha\alpha}$	ref	bond lengths, Å	ref
NF_4^+	848.2	443.3	1158.95	611.15	17	6.153	0.63			17	1.30(1)	18
PF_4^+	906	275	1167	358	10b	8.825	0.121			10b	1.480, 1.470[b]	98, 10b
AsF_4^+	748	272	825	287	3	5.76	0.16	0.31	0.02	84	1.606[c]	
NCl_4^+	635	430.3	283.3	233.3	19	2.86	0.32			19	1.764[b]	82
PCl_4^+	458	178	662	255	11	3.31	0.36	0.38	0.08	84	1.927(2)	12
$AsCl_4^+$	422	156	500	187	6a	3.22	0.17	0.22	0.02	84	2.0545(9)	4
$SbCl_4^+$	395.6	121.5	450.7	139.4	84	3.07	0.06	0.13	0.01	84	2.221(2)	84
$SnCl_4$[d]	369.1	95.2	408.2	126.1	99	2.55	0.10	0.11	0.02	94	2.280	78
$InCl_4^-$	321	89	337	112	100	1.77	0.13	0.08	0.02	94	2.350(3)	80
$CdCl_4^{2-}$	261	84	249, 240	98	101	1.03	0.14	0.07	0.00	94		
PBr_4^+	254	116	503, 496	148	14	2.15	0.30	0.29	0.04	84	2.17(1)	13
$AsBr_4^+$	244	88	349	115	7	2.29	0.16	0.47	0.02	84	2.221[c]	
$SbBr_4^+$	234.4	76.2	304.9	92.1	84	2.32	0.09	0.11	0.01	84	2.385(2)	84
$SnBr_4$[d]	222.1	59.4	284.0	85.9	99	2.01	0.10	0.09	0.02	94	2.40(3)	79
$InBr_4^-$	197	55	239	79	102	1.44	0.13	0.08	0.02	94	2.489(3), 2.479(3)	81, 80
$CdBr_4^{2-}$	161	49	177	75, 61	101	0.89	0.14	0.05	0.002	94	2.560	82
PI_4^+	193.5	71.0	410[e]	89.0	16	1.85	0.32	0.14	0.01	84	2.396(9)	15
AsI_4^+	183	72	319	87	8	2.17	0.11	0.13	0.00	84	2.449[c]	

[a] Stretching (f_r, f_{rr}) and bending (f_α, $f_{\alpha\alpha}$) force constants have units of mdyn $Å^{-1}$. [b] The bond lengths for NCl_4^+ and PF_4^+ are theoretical values. [c] The bond lengths of AsF_4^+, $AsBr_4^+$ and AsI_4^+ were estimated from plots of bond length vs electronegativity difference of the bonded atoms for a given group 15 element in PnX_4^+ and for its group 14 tetrahalide in the same row of the periodic table. Parallel behavior of each pair of plots enabled extrapolation to an unknown value. The electronegativity values calculated by Allen were used (Allen, L. C. *J. Am. Chem. Soc.* **1989**, *111*, 9003). In additional to the experimental PnX_4^+ cation bond lengths listed in this table, the following experimental values were used: $SnCl_4$, 2.280 Å; $SnBr_4$, 2.46 Å; SnI_4, 2.69 Å; GeF_4, 1.68 Å; $GeCl_4$, 2.113 Å; $GeBr_4$, 2.272 Å; GeI_4, 2.500 Å; SiF_4, 1.553 Å; $SiCl_4$, 2.019 Å; $SiBr_4$, 2.183 Å. [d] Gas phase Raman data. [e] The value for $\nu_3(T_2)$ was estimated from $\nu_3(T_2)$ of PCl_4^+; i.e. $\nu_3(T_2)$ $PI_4^+ = 0.62 \times \nu_3(PCl_4^+)$ (ref. (96)).

analyses of these and related PnX_4^+ cations. Earlier reports of normal coordinate analyses for $SbCl_4^+$ [89−95] are based on the erroneous assumption that the $SbCl_4F$ tetramer[26,27] was formulated as $SbCl_4^+F^-$ [25] (see **Introduction**).

As expected, the stretching frequencies decrease from $SbCl_4^+$ to $SbBr_4^+$ and from the antimony to the arsenic analog in accord with the reduced mass effect. The trends, $\nu_3(T_2) > \nu_1(A_1)$ and $\nu_4(T_2) > \nu_2(E)$, follow the trends observed for all tetrahedral halogen compounds, except $TlBr_4^-$ and UF_4 (Table 7).[96] The general valence force constants of the PI_4^+, AsF_4^+, $AsBr_4^+$, AsI_4^+, $SbCl_4^+$, and $SbBr_4^+$ cations, which have been calculated for the first time and the previously determined force constants for PF_4^+, PCl_4^+, PBr_4^+, and $AsCl_4^+$ (recalculated in the present study for the chloro and bromo cations) were determined using a GVFF[97] and are compared with those previously reported for the isoelectronic tetrahalides of row five (Table 7). The $SbCl_4^+$ and $SbBr_4^+$ cations fit into an existing trend among isoelectronic tetrahalides of the fifth row in which all four vibrational frequencies and their associated force constants decrease monotonically over the series $SbX_4^+ > SnX_4 > InX_4^- > CdX_4^{2-}$, reflecting the anticipated decrease in metal−halogen bond polarity and bond length with increasing positive charge. A general decrease in the valence force constant, f_r, occurs from PnF_4^+ to PnI_4^+. The interaction stretching force constants, f_{rr}, and bending force constants, f_α, show the usual monotonic decreases with increasing atomic number of the central atom. Bond order estimates for the series PX_4^+, AsX_4^+ and SbX_4^+ calculated from valence force constants using the empirical method of Siebert[95] indicate that the P−X, As−X, and Sb-X bond orders are greater than 1. The trend in the valence force constants of PCl_4^+ and PBr_4^+, has been explained in terms of $p\pi - d\pi$ bonding involving the d_{z^2} and $d_{x^2-y^2}$ pnicogen orbitals and halogen p-orbitals of appropriate symmetry. The larger f_r and larger calculated bond order of PCl_4^+ relative to that of PBr_4^+ have been attributed to contraction of the diffuse d-orbitals by the more electronegative chlorine ligands, but may also be accounted for in terms of energetically more favorable σ-orbitals for elements of the same row as well as ligand steric interactions (*vide infra*). Analogous trends are apparent for $NF_4^+-NCl_4^+$, $PF_4^+-PCl_4^+-PI_4^+$, $AsCl_4^+-AsBr_4^+-AsI_4^+$ and $SbCl_4^+-SbBr_4^+$. In contrast to the valence force constants of the PnF_4^+ and $PnCl_4^+$ series, which decrease with increasing atomic number of the pnicogen for P, As and Sb, the order is reversed for the $PnBr_4^+$ series and for $PI_4^+-AsI_4^+$, $NF_4^+-PF_4^+$, and $NCl_4^+-PCl_4^+$. There is also a leveling of valence force constants among the bromides so that f_r of $AsBr_4^+$ is essentially equal to that of $SbBr_4^+$. The trend reversals likely arise from increased ligand repulsion, which is most severe for PBr_4^+ and PI_4^+ and for NF_4^+ and NCl_4^+. The similarity of the As−Br and Sb−Br stretching force constants indicates that their bond energies are comparable. It has been noted,[90] and it is also

(89) Nagarajan, G.; Müller, A. *Z. Anorg. Allg. Chem.* **1967**, *349*, 82.
(90) Müller, A.; Fadini, A. *Z. Anorg. Allg. Chem.* **1967**, *349*, 164.
(91) Müller, A.; Krebs, B. *J. Mol. Spectrosc.* **1967**, *24*, 180.
(92) Wendling, E.; Mahmoudi, S. *Bull. Soc. Chim. Fr.* **1970**, *12*, 4248.
(93) Wendling, E.; Mahmoudi, S. *Bull. Soc. Chim. Fr.* **1971**, *1*, 3.
(94) Basile, L. J.; Ferraro, J. R.; LaBonville, P.; Wall, M. C. *Coord. Chem. Rev.* **1973**, *11*, 21.
(95) Siebert, H. *Anwendungen der Schwingungspektroskopie in der Anorganischen Chemie;* Anorganische und Allgemeine Chemie in Einzeldarstellungen 7; Springer Verlag: Berlin, 1966.
(96) Nakamoto, K. *Infrared and Raman Spectra of Inorganic and Coordination Compounds*, 4th ed.; J. Wiley & Sons: New York, 1986.
(97) Because the GVFF involves four frequencies and four force constants, a perfect fit of experimental frequencies is obtained and consequently the calculated frequencies are not given. Only four of the seven force constants in the GVFF are required to describe the forces taking place in a T_d molecule. The force constants associated with the stretch-bend ($f_{r\alpha'}$) and angle-angle- ($f_{\alpha\alpha'}$) interactions are assumed to be zero since the internal coordinates do not share a common bond. The interaction force constant, $f_{r\alpha}$, appears to have a negligible effect on the fit between observed and calculated values when the central atom is heavy[90] and is also assumed to be zero in this work. However, values reported for the phosphorus series of cations may be expected to exhibit significant couplings which are not accounted for in the present calculations for PCl_4^+, PBr_4^+, and PI_4^+. In addition to the diagonal constants f_r and f_α, the necessary interaction terms are f_{rr} and $f_{\alpha\alpha}$.
(98) O'Keeffe, M. *J. Am. Chem. Soc.* **1986**, *108*, 4341.
(99) Clark, R. J. H.; Mitchell, P. D. *J. Chem. Soc., Faraday Trans.* **1975**, *71*, 515.
(100) Woodward, L. A.; Taylor, M. J. *J. Chem. Soc.* **1960**, 4473.
(101) Goggin, P. L.; Goodfellow, R. J.; Kessler. K. *J. Chem. Soc., Dalton Trans.* **1977**, 1914.
(102) Woodward, L. A.; Bill, P. T. *J. Chem. Soc.* **1955**, 1699.

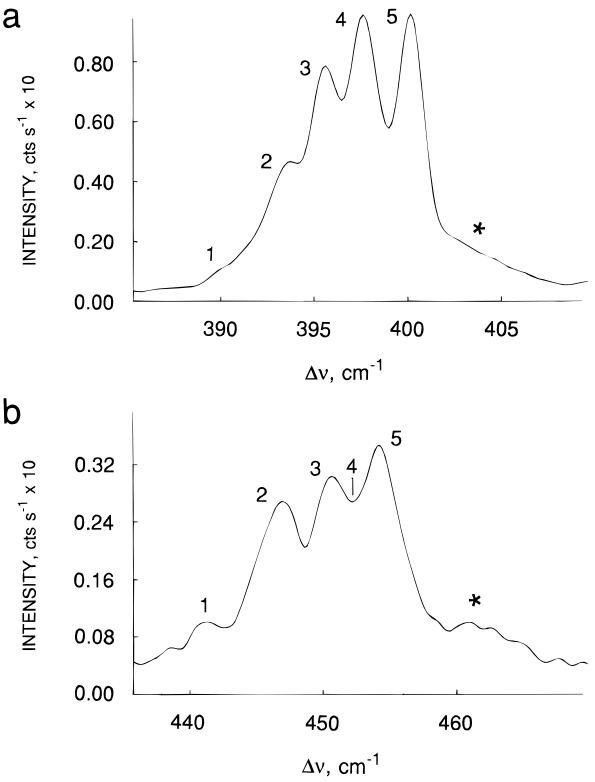

Figure 6. High-resolution Raman spectra (−160 °C) showing the natural abundance chlorine isotopic shifts of $SbCl_4^+Sb(OTeF_5)_6^-$ for (a) the $\nu_1(A_1)$ region (line 1, $Sb^{37}Cl_4^+$ (T_d); line 2, $Sb^{35}Cl^{37}Cl_3^+$ (C_{3v}); line 3, $Sb^{35}Cl_2^{37}Cl_2^+$ (C_{2v}); line 4, $Sb^{35}Cl_3^{37}Cl^+$ (C_{3v}); line 5, $Sb^{35}Cl_4^+$ (T_d)) and for (b) the $\nu_3(T_2)$ region (line 1, {[$\nu_8(B_2)$, $Sb^{35}Cl_2^{37}Cl_2^+$ (C_{2v})] + [ν_4(E), $Sb^{35}Cl^{37}Cl_3^+$ (C_{3v})] + [$\nu_3(T_2)$, $Sb^{37}Cl_4^+$ (T_d)]}; line 2, [$\nu_2(A_1)$, $Sb^{35}Cl^{37}Cl_3^+$ (C_{3v})]; line 3, [$\nu_2(A_1)$, $Sb^{35}Cl_2^{37}Cl_2^+$ (C_{2v})]; line 4, [$\nu_2(A_1)$, $Sb^{35}Cl_3^{37}Cl^+$ (C_{3v})], not resolved; line 5, {[$\nu_3(T_2)$, $Sb^{35}Cl_4^+$ (T_d)] + [ν_4(E), $Sb^{35}Cl_3^{37}Cl^+$ (C_{3v})] + [$\nu_6(B_1)$, $Sb^{35}Cl_2^{37}Cl_2^+$ (C_{2v})]}). Asterisks denote anion modes.

evident from the present work, that the force constants increase with formal oxidation state of the pnicogen, i.e., $PnX_4^+ > PnX_3$, reflecting the anticipated decrease in Pn−X bond polarity with increasing oxidation state of the pnicogen.

Splittings arising from the $^{35/37}Cl$ isotope effect are observed on $\nu_1(A_1)$ and $\nu_3(T_2)$ of the $SbCl_4^+$ cation (Figure 6) and are consistent with the essentially perfect T_d point symmetry of the cation and with the formal absence of a factor-group splitting on $\nu_1(A_1)$ and a factor-group splitting on $\nu_3(T_2)$ which is below resolution limits. It was not possible to resolve chlorine isotope patterns on the ν_2(E) and $\nu_4(T_2)$ bands, which are expected to be smaller and more difficult to resolve for low-frequency bending and stretching modes. Isotopic splittings have been observed for $\nu_1(A_1)$ and $\nu_3(T_2)$ of isoelectronic $SnCl_4$[103−106] as well as for the lighter group 14 tetrachlorides.[106−109] The isotopomer symmetries, their percent natural abundances and the symmetry species of their vibrational modes are given in Table 8. The isotopic splitting patterns of the $\nu_1(A_1)$ and $\nu_3(T_2)$ regions were assigned by analogy with those of matrix isolated $^{116}SnCl_4$ and $^{124}SnCl_4$.[105] The isotopic splitting pattern of five equally spaced lines in the $\nu_1(A_1)$ region are assigned, in order of increasing frequency, to the $\nu_1(A_1)$ modes of $Sb^{37}Cl_4^+$ (T_d) < $Sb^{35}Cl^{37}Cl_3^+$ (C_{3v}) < $Sb^{35}Cl_2^{37}Cl_2^+$ (C_{2v}) < $Sb^{35}Cl_3^{37}Cl^+$ (C_{3v}) < $Sb^{35}Cl_4^+$ (T_d) and have an average isotope shift per unit mass (is/*m*(Cl)) of 1.3 cm^{-1} amu^{-1} (Table 9). The nine bands in the chlorine isotope pattern in the $\nu_3(T_2)$ region of $SbCl_4^+$ are expected to partially overlap by analogy with those of $SnCl_4$ to give a five-peak chlorine isotope pattern arranged in the following order of increasing frequency: line 1 {[$\nu_8(B_2)$, $Sb^{35}Cl_2^{37}Cl_2^+$ (C_{2v})] + [ν_4(E), $Sb^{35}Cl^{37}Cl_3^+$ (C_{3v})] + [$\nu_3(T_2)$, $Sb^{37}Cl_4^+$ (T_d)]} < line 2 [$\nu_2(A_1)$, $Sb^{35}Cl^{37}Cl_3^+$ (C_{3v})] < line 3 [$\nu_2(A_1)$, $Sb^{35}Cl_2^{37}Cl_2^+$ (C_{2v})] < line 4 [$\nu_2(A_1)$, $Sb^{35}Cl_3^{37}Cl^+$ (C_{3v})] < line 5 {[$\nu_3(T_2)$, $Sb^{35}Cl_4^+$ (T_d)] + [ν_4(E), $Sb^{35}Cl_3^{37}Cl^+$ (C_{3v})] + [$\nu_6(B_1)$, $Sb^{35}Cl_2^{37}Cl_2^+$ (C_{2v})]}. In the experimental pattern, lines 1, 2, 3, and 5 are resolved having an is/*m*(Cl) value of 1.6 cm^{-1} amu^{-1}. The is/m(Cl) values are comparable to those reported for $SnCl_4$ (1.3 cm^{-1} amu^{-1}, $\nu_1(A_1)$ region, and 1.0 cm^{-1} amu^{-1}, $\nu_3(T_2)$ region).[105] Although antimony possesses two natural abundance isotopes, ^{121}Sb (57.25%) and ^{123}Sb (42.75%), the $\nu_1(A_1)$ modes are expected to be insensitive to the antimony isotopic effect. The insensitivity results from zero (T_d) or nearly zero (C_{3v} and C_{2v}) vibrational amplitudes of the antimony atom in normal modes of A_1 symmetry in the $\nu_1(A_1)$ region [cf. is/*m*(Sn) = 0 for $\nu_1(A_1)$ (T_d) of $^{116}Sn^{35}Cl_4$−$^{124}Sn^{35}Cl_4$ and $^{116}Sn^{37}Cl_4$−$^{124}Sn^{37}Cl_4$ and for $\nu_1(A_1)$ (C_{3v}) of $^{116}Sn^{35}Cl_3^{37}Cl$−$^{124}Sn^{35}Cl_3^{37}Cl$]. The antimony isotopic shift is too small to be resolved in the $\nu_3(T_2)$ region and does not result in line broadening sufficient to obscure the chlorine isotopic splittings in this region. The size of the antimony isotopic splitting on $\nu_3(T_2)$ of $SbCl_4^+$, which possesses less polar metal−chlorine

Table 8. Vibrational Bands and Activities of the $Sb^{35}Cl_n^{37}Cl_{4-n}^+$ Cation[a]

isotopomer	point sym	%	ν_1[b]	ν_2	ν_3[b]	ν_4
$Sb^{35}Cl_4^+$	T_d	32.5	A_1	E	T_2	T_2
$Sb^{35}Cl_3^{37}Cl^+$	C_{3v}	42.2	A_1	E	$A_1 + E$	$A_1 + E$
$Sb^{35}Cl_2^{37}Cl_2^+$	C_{2v}	20.5	A_1	$A_1 + A_2$	$A_1 + B_1 + B_2$	$A_1 + B_1 + B_2$
$Sb^{35}Cl^{37}Cl_3^+$	C_{3v}	4.4	A_1	E	$A_1 + E$	$A_1 + E$
$Sb^{37}Cl_4^+$	T_d	0.4	A_1	E	T_2	T_2
total no. of bands			5	6	9	9

[a] All modes for all symmetries are Raman active. With the exception of the A_1 and E modes under T_d symmetry, all other modes are IR active. [b] Chlorine isotope splittings in $SbCl_4^+$ were large enough to be resolved on these modes (see Table 9).

Table 9. Raman Frequencies for the Chlorine Isotopic Splittings on $\nu_1(A_1)$ and $\nu_3(T_2)$ of $SbCl_4^+$ and Their Assignments

assignment	frequencies, cm^{-1}
$\nu_1(A_1)$ region	
$\nu_1(A_1)$, $Sb^{35}Cl_4^+$	400.2
$\nu_1(A_1)$, $Sb^{35}Cl_3^{37}Cl^+$	397.6
$\nu_1(A_1)$, $Sb^{35}Cl_2^{37}Cl_2^+$	395.6
$\nu_1(A_1)$, $Sb^{35}Cl^{37}Cl_3^+$	393.7
$\nu_1(A_1)$, $Sb^{37}Cl_4^+$	390.4
$\nu_3(T_2)$ region	
$\nu_3(T_2)$, $Sb^{35}Cl_4^+$; ν_4(E), $Sb^{35}Cl_3^{37}Cl^+$; $\nu_6(B_1)$, $Sb^{35}Cl_2^{37}Cl_2^+$	454.2
$\nu_2(A_1)$, $Sb^{35}Cl_3^{37}Cl^+$	
$\nu_2(A_1)$, $Sb^{35}Cl_2^{37}Cl_2^+$	450.8
$\nu_2(A_1)$, $Sb^{35}Cl^{37}Cl_3^+$	446.9
$\nu_3(T_2)$, $Sb^{37}Cl_4^+$; ν_4(E), $Sb^{35}Cl^{37}Cl_3^+$; $\nu_8(B_2)$, $Sb^{35}Cl_2^{37}Cl_2^+$	441.7

(103) Müller, A.; Königer, F.; Nakamoto, K.; Ohkaku, N. *Spectrochim. Acta* **1972**, *28A*, 1933.
(104) Shurvell, H. F. *Can. J. Spectrosc.* **1972**, *17*, 109.
(105) Königer, F.; Müller, A. *J. Mol. Spectr.* **1975**, *56*, 200.
(106) Chumaevskii, N. A. *Russ. J. Inorg. Chem.* (*Engl. Transl.*) **1991**, *36*, 1491.
(107) King, S. T. *J. Chem. Phys.* **1968**, *49*, 1321.
(108) Königer, F.; Müller, A.; Nakamoto, K. *Z. Naturforsch.* **1975**, *30b*, 456.
(109) Tevault, D.; Brown, J. D.; Nakamoto, K. *Appl. Spectrosc.* **1976**, *30*, 461.

bonds, is expected to be less than that determined for $\nu_3(T_2)(T_d)$ of $^{116}Sn^{35}Cl_4-^{124}Sn^{35}Cl_4$ and $^{116}Sn^{37}Cl_4-^{124}Sn^{37}Cl_4$, where is/$m(Sn) = 0.5$ cm^{-1}.[105] Splittings arising from the $^{79/81}$Br isotope effect could not be resolved for $SbBr_4^+$.

Conclusions

The known $SbCl_4^+$ and novel $SbBr_4^+$ cations have been synthesized as their $Sb(OTeF_5)_6^-$ salts and are thermodynamically stable with respect to decomposition to $Sb(OTeF_5)_3$ and X_2. The $SbBr_4^+$ cation represents only the second tetrahalostibonium(V) cation to have been prepared and structurally characterized. The ready loss of Br_2 from $SbBr_4^+$ and ease of preparing the salt suggest that it may well become a valuable electrophilic brominating agent. The crystal structures of both salts show significantly fewer and weaker interactions between the anion and the cation than in previously known $SbCl_4^+$ salts, and in $SbCl_4^+$ and $SbBr_4^+$ cations which are undistorted from their ideal tetrahedral geometries. The first NMR chemical shifts of any tetrahalocation of a heavy pnicogen (As, Sb, or Bi) have been obtained for $SbCl_4^+$ and $SbBr_4^+$ in SO_2ClF solvent. General valence force constant calculations for all known tetrahalonium cations of group 15 are given and the trends in valence force constants $PBr_4^+ < AsBr_4^+ < SbBr_4^+$, $PI_4^+ < AsI_4^+$, $NCl_4^+ < PCl_4^+$, $NF_4^+ < PCl_4^+$ show that bond strengths decrease with decreasing atomic mass of the group 15 atom and suggest that increased ligand repulsions are likely a significant contributing factor.

Experimental Section

Materials and Apparatus. Manipulations involving volatile materials were performed under strictly anhydrous conditions on a Pyrex glass vacuum line equipped with grease free glass/Teflon stopcocks (J. Young Scientific Glassware). Glass reaction vessels, unless otherwise noted, were joined to Young valves through $^1/_4$ in. o.d. lengths of glass tubing fused to the valve and the reaction vessel using $^1/_4$ in. stainless steel Cajon Ultra-Torr unions fitted with Viton O-rings. All reaction vessels were dried under dynamic vacuum for a minimum of 10 h prior to use. Reaction vessels constructed of $^1/_4$ in. o.d. FEP tubing and joined to Kel-F valves by means of 45° compression flares were similarly dried followed by passivation with 1 atm of F_2 gas overnight. Nonvolatile materials were handled in the dry nitrogen atmosphere of a glovebox (Vacuum Atmospheres Model DLX).

The reagents $HOTeF_5$,[110] $B(OTeF_5)_3$[111] and $Sb(OTeF_5)_3$[112] were prepared as described previously. Acetonitrile (Caledon HPLC Grade)[113] and SO_2ClF (Columbia Organic Chem. Co.)[114] were purified using literature methods and were condensed into reaction tubes and NMR sample tubes at −196 °C using a grease-free glass vacuum line. Antimony trifluoride (Aldrich, 98%) was sublimed under dynamic vacuum at ca. 200 °C prior to use and stored in a dry PFA bottle inside the drybox. Chlorine gas was dried by passing commercial Cl_2 (Matheson) through concentrated sulfuric acid, followed by condensation at −78 °C in a dry glass U-tube equipped with J. Young stopcocks and stored at −78 °C until used. Dry Cl_2 was metered out on the metal vacuum line which had been twice passivated with ca 1.5 atm of dry Cl_2 for 2 h prior to use. Dry bromine (Fischer; stored over P_4O_{10}) was used directly and was distilled from the glass storage ampule to a graduated glass tube (0.1 mL graduations), which was reweighed after each transfer of Br_2 to a reaction vessel. Iodine (BDH Chemical, 99.9%) was dried prior to use by triple sublimation from mixtures with BaO (Aldrich). Tetraethylammonium bromide (Aldrich) was dried under vacuum at 120 °C for 2 days prior to use.

(110) Sladky, F. *Inorganic Syntheses*; Shreeve, J. M., Ed., Wiley-Interscience: New York, 1986; Vol. 24, p 34.
(111) Kropshofer, H.; Leitzke, O.; Peringer, P.; Sladky, F. *Chem. Ber.* **1981**, *114*, 2644.
(112) Lentz, D.; Seppelt, K. *Z. Anorg. Allg. Chem.* **1983**, *502*, 83.
(113) Winfield, J. M. *J. Fluorine Chem.* **1984**, *25*, 91.
(114) Schrobilgen, G. J.; Holloway, J. H.; Granger, P.; Brevard, C. *Inorg. Chem.* **1978**, *17*, 980.

$SbCl_4^+Sb(OTeF_5)_6^-$ and $SbBr_4^+Sb(OTeF_5)_6^-$. Syntheses and Crystal Growing. $SbCl_4^+Sb(OTeF_5)_6^-$. In the drybox, 1.7447 g (2.083 mmol) of $Sb(OTeF_5)_3$ was loaded into a 10-mm standard wall glass tube and Cl_2 (4.182 mmol, 101 mol % excess) was condensed from a calibrated manifold into the tube at −196 °C. The tube was heat sealed under dynamic vacuum while the contents were kept frozen at −196 °C. Upon warming of the mixture to room temperature, a yellow liquid resulted. The tube was mounted horizontally and within several hours, the formation of small, well-formed crystals was observed. After 4 days, a white, crystalline mass had formed. The tube was transferred to the drybox and the bottom cooled to −150 °C in order to freeze the excess chlorine, the tube was cut open and a glass/Teflon valve was attached to a stainless steel $^1/_4$ in. Cajon union. The tube was removed from the drybox, connected to the vacuum line and the excess of chlorine pumped off at −78 °C. The tube was returned to the drybox and reweighed. The mass of the white solid was 1.8966 g, giving a molar ratio $Sb(OTeF_5)_3$:Cl_2 of 1:1.028.

In order to obtain crystals suitable for X-ray crystallography, a stoichiometric excess of $Sb(OTeF_5)_3$ was used as solvent. The following amounts of reactants were used: 0.8189 g (0.978 mmol, 22 mol % excess) of $Sb(OTeF_5)_3$ and 0.802 mmol of Cl_2. The sealed glass tube was mounted horizontally inside the fumehood and left undisturbed. Colorless crystals began to appear overnight, and the tube was left undisturbed until the contents had completely decolorized. The tube was transferred to the drybox and cut open, and well-formed crystals were separated from the surrounding material. The crystals were transparent hexagonal parallelepipeds and several were mounted and sealed inside 0.3−0.5 mm glass Lindemann capillaries.

$SbBr_4^+Sb(OTeF_5)_6^-$. In a typical preparation, 2.1131 g (2.523 mmol) of $Sb(OTeF_5)_3$ was loaded into a $^1/_4$ in. o.d. FEP tube equipped with a 316 stainless steel valve (Whitey SS-ORM2) in the drybox. The tube was removed from the drybox and connected to the vacuum line, and 0.4587 g (2.870 mmol, 13 mol % excess) of Br_2 was distilled onto the solid at −196 °C. On warming to room temperature, the contents of the tube melted to give a red-brown solution of Br_2 in $Sb(OTeF_5)_3$ solvent and undissolved bromine. The tube was mounted horizontally and after several hours, crystal growth was observed. The tube was agitated several times to effect complete reaction and after 5 days, a yellow, microcrystalline powder had formed. The excess of Br_2 was removed under dynamic vacuum and the tube was transferred into the drybox, the valve removed and the tube weighed. The mass of the solid was 2.5129 g, giving a molar ratio $Sb(OTeF_5)_3$:Br_2 of 1:0.997. The tube was closed with a stainless steel cap and stored in the drybox.

The procedure for crystal growth was similar to that described above for the preparation of $SbBr_4^+Sb(OTeF_5)_6^-$ except that a larger excess of Br_2 was used. The following amounts of reactants were used: 1.1345 g (1.355 mmol) of $Sb(OTeF_5)_3$ and 0.2616 g (1.637 mmol, 21 mol % excess) of Br_2. The FEP tube was mounted horizontally and left undisturbed. After one week, the sample completely solidified to give a yellow crystalline mass. Excess Br_2 was carefully removed under vacuum and the tube transferred to the drybox, opened, and weighed. The weight of the product was 1.3552 g, giving a molar ratio $Sb(OTeF_5)_3$:Br_2 of 1:1.001. The crystals were large yellow hexagonal prisms and had to be cut with a scalpel in order to be mounted and sealed inside 0.5 mm glass Lindemann capillaries.

Crystals of both salts were stored at −10 °C prior to mounting on the diffractometer. A preliminary examination of the extinctions of the sealed crystals under a polarizing microscope suggested that all crystals were single. The crystals used in this study had the dimensions $0.4 \times 0.5 \times 0.24$ mm^3 ($SbBr_4^+$) and $0.58 \times 0.5 \times 0.22$ mm^3 ($SbCl_4^+$).

Attempted Preparation of $SbI_4^+Sb(OTeF_5)_6^-$. In the drybox, 1.7773 g (2.122 mmol) of $Sb(OTeF_5)_3$ was loaded into a $^1/_4$ in. o.d. FEP tube equipped with a 316 stainless steel valve (Whitey SS-ORM2). The reaction tube was transferred from the drybox to a dry nitrogen filled glovebag where 0.6378 g (2.513 mmol, 12 mol % excess) of I_2 was added. When mixed at room temperature, the contents of the tube liquified to give a dark violet solution of I_2 in $Sb(OTeF_5)_3$ and undissolved crystalline iodine. The tube was allowed to stand for several weeks with periodic mixing, but no reaction was observed.

Decomposition of $SbBr_4^+Sb(OTeF_5)_6^-$ in CH_3CN and SO_2ClF Solvents and in the Presence of Br^-. In the drybox, 1.3180 g (0.661 mmol) of $SbBr_4^+Sb(OTeF_5)_6^-$ was loaded into a 10-mm medium wall

glass tube. The tube was attached to a Young valve, removed from the drybox and connected to the glass vacuum line. Anhydrous CH_3CN (ca. 3 mL) was condensed onto the solid at −196 °C. When warmed to −40 °C, the solvent liquefied and the contents of the tube immediately took on a deep red-brown color. The tube was warmed and left at room temperature for ca. 30 min. The tube and contents were then cooled in ice and the volatiles removed *in vacuo*. After ca. 20 min, a solid mass had formed at the bottom of the tube, which occluded some solvent. In order to completely remove the solvent, the tube was warmed to ca. 35−40 °C. After overnight pumping, a white powder remained in the tube and some colorless crystals had formed at the top of the tube and in the Young valve. The tube was removed from the vacuum line and immediately transferred into the drybox and weighed. The weight of the product (1.2641 g compared to 1.2124 g, the weight expected for 0.661 mmol of $SbBr_2^+Sb(OTeF_5)_6^-$) suggested that some solvent was still present in the solid. Some of the colorless crystals were sealed in melting point capillaries for Raman spectroscopy and X-ray crystallography which revealed they were $SbBr_3$.[37,38] The bulk sample was examined by ^{19}F and ^1H NMR in SO_2ClF solvent (see **Results and Discussion**) and by Raman spectroscopy (cm^{-1}): ν(C≡N), 2315(4), 2307(2), 2287(5), 2277(3); $\delta(CH_3)$, 1444(<1), 1413(<1); ν(C-C), 1300(2); ν_8(E), $\nu_{as}(TeF_4)$, 720(2); $\nu_1(A_1)$, ν_s(TeF), 715(2), 703(13), 698(6, sh); $\nu_2(A_1)$, $\nu s(TeF_4)$, 662(23); $\nu_5(B_1)$, $\nu_{as}(TeF_4)$, 646(4), 636(2); $\nu_3(A_1)$, ν_s(TeO), 403(5); ? 365(<1); $\nu_4(A_1)$, $\nu_s(FTeF_4)$, 304(3), 282(3); ν(SbBr), 241(13), 236(92); $\nu_7(B_2)$, $\delta_{sciss}(TeF_4)$, 231(6); ν(SbBr), 227(100), 222(9), 216(5); δ(TeOSb), 141-(3); δ(BrSbBr), 111(27); δ(BrSbBr), 93(27), 85(17). The presence of free or coordinated $SbBr_2^+$ is not unambiguously established by Raman spectroscopy as its three Raman bands (cm^{-1}) in $SbBr_2^+GaBr_4^-$ [$\nu_1(A_1)$, ν_s(SbBr), 240 (100); $\nu_3(B_2)$, ν_{as}(SbBr), 235 (25, sh); $\nu_2(A_1)$, δ_s-(BrSbBr), 128 (11); $\nu_3-\nu_2$, 105 (6)][36] are similar to those of $SbBr_3$ [$\nu_1(A_1)$, ν_s(SbBr), 235 (100), 241 (15); ν_3(E), ν_{as}(SbBr), 217 (8), 220 (18, sh), 227(89); $\nu_2(A_1)$, δ_s(BrSbBr), 109 (37); ν_4(E), δ_{as}(BrSbBr), 93 (38), 85(26)].[37]

In a related experiment, 0.5253 g (0.2634 mmol) of $SbBr_4^+Sb(OTeF_5)_6^-$ was loaded into a 8-mm tube glass blown to a Young valve and ca. 1.5 mL of SO_2ClF condensed in at −196 °C. The tube and contents were allowed to stand at room temperature for 8 days whereupon Br_2 was slowly liberated, turning the solution from yellow to red-brown. Slow removal of the solvent at room temperature resulted in a yellow crystalline solid (0.4989 g). The Raman spectrum revealed that the solid consisted mainly of $SbBr_4^+Sb(OTeF_5)_6^-$. The ^{19}F NMR spectrum of the residue redissolved in SO_2ClF showed an intense (ca. 80% of the total integrated ^{19}F intensity) AB_4 pattern assigned to the $Sb(OTeF_5)_6^-$ anion (see **Results and Discussion. NMR Spectroscopy**) and a weak (ca. 20%), less severe AB_4 pattern [$\delta(^{19}F_A)$, −41.3 ppm; $\delta(^{19}F_B)$, −38.2 ppm and $^1J(^{19}F_A-^{19}F_B)$, 175 Hz; $^1J(^{19}F_A-^{125}Te)$, 3455 Hz; $^1J(^{19}F_B-^{125}Te)$, 3616 Hz] which presently cannot be assigned. The Raman spectrum appeared identical to that of $SbBr_4^+Sb(OTeF_5)_6^-$ (see **Results and Discussion. Raman Spectroscopy**).

In a drybox, 0.185 82 g (0.0932 mmol) of $SbBr_4^+Sb(OTeF_5)_6^-$ was loaded into a 1/4 in. o.d. glass tube, cooled to ca. −130 °C, and 0.015 38 g (0.0998 mmol) of dry $N(CH_2CH_3)_4^+Br^-$ was added. The reaction tube was closed by a 4-mm Young valve attached to a 1/4-in. stainless steel Cajon union, removed from the drybox, and SO_2ClF was condensed onto the solid mixture at −196 °C. Upon warming of the mixture from −78 to −60 °C, Br_2 formed, and after 1 h the sample was pumped to dryness, yielding a white powder weighing 0.186 37 g. The weight loss (0.014 83 g) corresponded to 0.0932 mmol of Br_2.

Attempted Halogen Exchange between $SbCl_4^+$ and $SbBr_4^+$. To a 10-mm glass NMR tube in the drybox were added 0.1544 g (0.0994 mmol) of $SbCl_4^+Sb(OTeF_5)_6^-$ and 0.1912 g (0.0959 mmol) of $SbBr_4^+Sb(OTeF_5)_6^-$, ca. 2.5 mL of SO_2ClF was condensed into the tube at −196 °C, and the sample was heat sealed. The solutes dissolved at −78 °C, and the light yellow sample was stored at this temperature until its ^{121}Sb and ^{123}Sb NMR spectra could be obtained.

Crystal Structure Determinations of $SbCl_4^+Sb(OTeF_5)_6^-$ and $SbBr_4^+Sb(OTeF_5)_6^-$. Collection and Reduction of X-ray Data. The crystals of the chlorine and bromine compounds were centered on a Siemens/Syntex P3 diffractometer, using silver radiation monochromatized with a graphite crystal (λ = 0.560 86 Å). The experimental values for the bromine compound, when they differ from those of the chlorine compound, are given in square brackets. The data sets were collected at −75 °C [−81 °C]. During data collection, the intensities of three standard reflections were monitored every 97 reflections to check for crystal stability and alignment. No decay was observed. Accurate cell dimensions were determined at −75 °C [−81 °C] from a least-squares refinement of the setting angles (χ, ϕ, and 2θ) obtained from 26 [36] accurately centered reflections (with 15.42° [15.16°] ≤ 2θ ≤ 34.51° [30.17°]) chosen from a variety of points in reciprocal space. The examination of the peak profiles revealed only single peaks. Integrated diffraction intensities were collected using a $\theta-2\theta$ scan technique with scan rates varying from 2.003 [1.5] to 14.65 deg/min (in 2θ) so that the weaker reflections were examined most slowly to minimize counting errors. The data were collected with −15 [−15] ≤ h ≤ 0, 0 ≤ k ≤ 15 [15], and −23 [0] ≤ l ≤ 28 [29] and with 3° ≤ 2θ ≤ 50° [50°]. A total of 6823 [5092] reflections were collected out of which 213 [162] were standard reflections. After averaging of equivalent reflections, 3969 [4177] unique reflections remained. A total of 3617 [3444] reflections, satisfying the condition $I \geq 2\sigma(I)$, were used for structure solution. Corrections were made for Lorentz and polarization effects. An empirical absorption correction was applied to the data by using the PSI SCAN method ($\Delta\phi$ = 10°) (μR = 0.805 [1.136]). The transmission factors ranged from 0.964 [0.467] to 0.481 [0.218].

Crystal Data. $Cl_4F_{30}O_6Sb_2Te_6$ (fw = 1816.90): crystallizes in the trigonal system $P\bar{3}$; a = 10.022(1) Å, c = 18.995(4) Å; V = 1652.3(6) Å^3; D_{calc} = 3.652 g cm^{-3} for Z = 2. Ag Kα radiation (λ = 0.56086 Å, μ(Ag Kα) = 38.7 cm^{-1}) was used. $Br_4F_{30}O_6Sb_2Te_6$ (fw = 1994.74): crystallizes in the trigonal system $P\bar{3}$; a = 10.206(1) Å, c = 19.297(3) Å; V = 1740.9(5) Å^3; D_{calc} = 3.806 g cm^{-3} for Z = 2. Ag Kα radiation (λ = 0.560 86 Å, μ(Ag Kα) = 59.8 cm^{-1}) was used.

Solution and Refinement of the Structures. The refinements of the two structures were identical; consequently the numerical values for the bromine compound, when they differ from those of the chlorine compound, are given in square brackets. The program XPREP[115] was used for confirming the correct cells and space groups. The five space groups which were consistent with the systematic absences were the centrosymmetric $P\bar{3}$ and $P\bar{6}/m$ space groups, the chiral $P\bar{3}$ and $P\bar{6}$ space groups and the non-centrosymmetric $P\bar{6}$ space group. Even though the E-statistics (calculated, 0.738 [0.739]; theoretical, 0.736) suggested a noncentrosymmetric space group, the structure was solved in the space group $P\bar{3}$ (R_{int} = 0.040 [0.021]) which proved to be the right space group. A first solution was obtained without absorption corrections by direct methods which located the antimony and halogen atoms of the cation (Sb atom and one halogen atom on special position (3..) and one halogen atom on general position), the special positions ($\bar{3}$) of the Sb atoms of the two anions, and the general positions of the Te atoms of the two anions. The full-matrix least-squares refinement of all the above atom positions and isotropic thermal parameters gave a conventional agreement index R of 0.327 [0.331]. A difference Fourier synthesis revealed the remaining general positions of all fluorine and oxygen atoms. The introduction of these positions gave a residual factor of 0.294 [0.308]. Surprisingly, the introduction of anisotropic thermal parameters for all the heavy atoms did not improve the residual, but uncertainties in coordinates, bond lengths, and bond angles were reduced. Such behavior suggested that the crystal was a merohedral twin, which can be expected in a trigonal system. Twin domains of this type have the same lattice in the parallel orientation, i.e., the reciprocal lattices coincide, which was observed for both compounds. The two twin laws which are most commonly expected in a trigonal system are (100 010 $\bar{1}0\bar{1}$) and (100 010 $00\bar{1}$). A refinement was carried out using both laws; in the first case, the residual remained the same, while with the second law, the residual dropped drastically to 0.0934 [0.1123], indicating it was the correct twin law. The structure was then solved using data that had been corrected empirically for absorption, and all the heavy atoms refined with anisotropic thermal parameters (R = 0.0604 [0.0741]). The final refinement twin ratio was 53/47 [47/53]. At this point, it was possible to distinguish a significant difference between the values of the thermal parameters of

(115) Sheldrick, G. M. SHELXTL PLUS, Release 4.21/V; Siemens Analytical X-ray Instruments Inc.: Madison, WI, 1993.

the oxygen and fluorine atoms of the two anions, as well as the Sb(2)−O(1)−Te(1) and Sb(3)−O(2)−Te(2) angles, respectively, suggesting the "Sb(3)" anion was disordered. The oxygen and fluorine atoms of the "Sb(2)" anion were easily refined anisotropically, while the program suggested the light atom positions of the "Sb(3)" anion were separated by 0.49 [0.72] Å. The disorder could be described as an orientational disorder involving two anions sharing the same central antimony atom and the same tellurium atoms in which the oxygen and the fluorine atoms were separated by 0.49 [0.72] Å. The structure was solved using a disorder model in which the Sb(3)−O, O−Te(2), and Te(2)−F distances were restrained to those in the "Sb(2)" anion, the O−Sb(3)−O, O−Te(2)−O, and F−Te(2)−F angles were restrained to 15° [21°], and the site occupancy factor was allowed to refine. The value of 15° [21°] was arrived at after solving the structure for different angle values and corresponded to the minimum *R* value. As expected, the introduction of the two partial positions was accompanied by a decrease in the values of the thermal parameters and, more importantly, by better agreement of the Sb−O−Te angles in the two anions (see Table 4). The site occupancy factors refined to a 51/49 [54/46] disorder. The final refinement was obtained by setting the weight factor to $1/[\sigma^2(F_o^2) + (0.079\ [0.0662]P)^2 + 6.443\ [0.000]P]$ and gave rise to a residual, R_1, of 0.0461 ($wR_2 = 0.1223$) [0.0425 (0.1014)]. In the final difference map, the maximum and the minimum electron densities were 8.49 [2.59] and −1.62 [−1.79] e Å^{-3}.

All calculations were performed on a 486 personal computer using the SHELXTL PLUS package[115] for structure determination, refinement and molecular graphics.

Nuclear Magnetic Resonance Spectroscopy. Nuclear magnetic resonance spectra were recorded unlocked (field drift < 0.1 Hz h^{-1}) on Bruker AC-300 (7.0463 T) and AM-500 (11.744 T) spectrometers equipped with Aspect 3000 computers. The ^{1}H and ^{19}F NMR spectra were obtained using a 5-mm ^{1}H/^{13}C/^{19}F/^{31}P combination probe. The ^{121}Sb and ^{123}Sb NMR spectra were obtained by using broad-band VSP probes tunable over the frequency ranges 14−122 MHz (AC-300) and 23−202 MHz (AM-500). The ^{121}Sb (119.696 MHz) and ^{123}Sb (64.820 MHz) NMR spectra of $SbBr_4^+Sb(OTeF_5)_6^-$ were recorded at 11.744 T using pulse widths of 15 and 17 μs, respectively, and correspond to a bulk magnetization tip angle of ∼90°. A total of 1200 and 1000 transients were acquired in 16K memories using spectral width settings of 15 and 25 kHz, acquisition times of 0.541 and 0.328 s, data point resolutions of 1.85 and 3.05 Hz/data point and a line broadening for the exponential smoothing of the free induction decays of 5 Hz for ^{123}Sb and ^{121} Sb, respectively. The ^{121}Sb (71.830 MHz) and ^{123}Sb (38.899 MHz) NMR spectra recorded at 7.0463 T were acquired using ∼90° pulse widths of 10.5 and 19 μs, respectively. The spectra were acquired in 64K and 16K memories using spectral width settings of 100 and 25 kHz, acquisition times of 0.164 and 0.328 s, a data point resolution of 3.05 Hz/data point and a line broadening of 5 Hz for $SbCl_4^+Sb(OTeF_5)_6^-$ (^{121}Sb, 2000 transients; ^{123}Sb, 6050 transients in SO_2ClF solvent and ^{121}Sb, 83 000 transients in CH_3CN solvent) and $SbBr_4^+Sb(OTeF_5)_6^-$ (^{121}Sb, 4100 transients; ^{123}Sb, 5000 transients), respectively. The ^{19}F NMR spectra were recorded at 282.408 MHz; 500 transients were acquired in 128K memories using a ∼90° pulse width of 1 μs, spectral width settings of 10 kHz, acquisition times of 1.64 s, and data point resolutions of 0.153 Hz/data point. Proton spectra were recorded at 300.134 MHz; 220 transients were acquired in 32K memories using a ∼90° pulse width of 2 μs, spectral width settings of 10 kHz, acquisition times of 0.819 s, and data point resolutions of 0.610 Hz/data point. No line broadening parameter was used when processing the ^{1}H and ^{19}F free induction decays, and no relaxation delays were used for any of the spectral acquisitions. The respective nuclei were referenced to neat samples of $CFCl_3$ (^{19}F) and $Si(CH_3)_4$ (^{1}H) and to a 1.00 M solution of $N(CH_2CH_3)_4^+SbF_6^-$ in CH_3CN (^{121}Sb and ^{123}Sb) at the sample temperatures for ^{121}Sb and ^{123}Sb spectra (see Table 1) and at 30 °C for ^{1}H and ^{19}F spectra. The chemical shift convention used was that a positive (negative) sign signifies a chemical shift to higher (lower) frequency with respect to the reference sample.

Spectra were recorded in 5-mm (^{19}F and ^{1}H) and 10-mm (^{121}Sb and ^{123}Sb) thin wall precision glass tubes (Wilmad). Following condensation of SO_2ClF or CH_3CN solvent into the sample tube at −196 °C, the sample tubes were heat sealed under dynamic vacuum while the contents were kept frozen at −196 °C.

Raman Spectroscopy. Raman spectra were recorded on a Jobin-Yvon Mole S-3000 triple spectrograph system equipped with a 0.32-m prefilter, an adjustable 25-mm entrance slit, and a 1.00-m monochromator. The instrument settings for the bromine compounds, when they differ from those of the chlorine compound, are given in square brackets. Holographic gratings were used for the prefilter (600 grooves mm^{-1}, blazed at 500 nm) and monochromator (2400 grooves mm^{-1}, blazed at 550 nm) stages. The 514.5 nm line of a Spectra Physics Model 2016 Ar^+ ion laser was used for excitation of the samples. Spectra were recorded at −150 °C [−152 °C] on powdered microcrystalline samples in 5-mm o.d. thin wall Pyrex glass NMR tubes using the macrochamber of the instrument. Low temperatures were achieved by flowing dry N_2 gas, chilled by passing through a 50-L tank of liquid nitrogen, along the outside of the sample tube, which was mounted vertically in an open-ended unsilvered glass Dewar jacket, and checked by placing a copper-constantan thermocouple wire (error, ±0.8 °C) in the sample region. A Spectraview-2D CCD detector equipped with a 25-mm chip (1152 × 298 pixels) was used for signal averaging. The Raman spectrometer was frequency calibrated using the 1018.3 or 730.4 cm^{-1} line of neat indene, which was sealed in a $^1/_4$ in. glass tube. The laser power was adjusted to 300 [500] mW at the sample. Slits were set to 100 μm (band pass, 2 cm^{-1}) for low-resolution spectra and 50 μm (band pass, 1 cm^{-1}) for resolution of $^{35/37}$Cl isotopic shifts in $SbCl_4^+Sb(OTeF_5)_6^-$. A total of 20 reads having 30 [20] s integration times were summed for the Raman spectra of $SbBr_4^+Sb(OTeF_5)_6^-$ and $(SbBr_2{\cdot}CH_3CN)^+Sb(OTeF_5)_6^-$. Owing to the high scattering powers of neat $SbBr_3$, the spectrum of this compound was obtained by summing 10 scans having 10 s integration times.

The force constants for $SbCl_4^+$, $SbBr_4^+$ and related tetrahalonium cations of group 15 were determined using a GVFF and the program SVIB.[116] All calculations were carried out on a Silicon Graphics 4600PC computer.

Acknowledgment. We thank the donors of the Petroleum Research Fund, administered by the American Chemical Society, for support of this work under Grant ACS-PRF No. 26192-AC3 (G.J.S.), the Natural Sciences and Engineering Research Council of Canada for a research grant (G.J.S.) and for the award of a graduate scholarship (N.L.), NATO for the award of a postdoctoral fellowship (W.J.C.), and the German Academic Exchange Service (DAAD) for the award of a travel grant (P.K.). We also thank Mr. Robert P. Hammond, Department of Chemistry, McMaster University, for his assistance in recognizing merohedral twinning in the title compounds.

Supporting Information Available: Structure determination parameters (Table 10), bond lengths and bond angles (Table 11), and anisotropic thermal parameters (Table 12) (8 pages). Ordering information is given on any current masthead page.

IC950818Z

(116) Mukherjee, A.; Spiro, T. G. SVIB program 656, Bulletin 15(1). Quantum Chemistry Program Exchange, Indiana University, 1995.